NATIONAL ADVISORY COMMITTEE FOR AERONAUTICS

TECHNICAL NOTE 4340

WIND-TUNNEL INVESTIGATION OF THE HIGH-SUBSONIC STATIC LONGITUDINAL STABILITY CHARACTERISTICS OF SEVERAL WING-BODY CONFIGURATIONS DESIGNED FOR HIGH LIFT-DRAG RATIOS AT A MACH NUMBER OF 1.4

By Paul G. Fournier

Langley Aeronautical Laboratory
Langley Field, Va.

NACA

Washington

July 1958

NATIONAL ADVISORY COMMITTEE FOR AERONAUTI

TECHNICAL NOTE 4340

WIND-TUNNEL INVESTIGATION OF THE HIGH-SUBSONIC STATIC LONGITUDINAL STABILITY CHARACTERISTICS OF SEVERAL WING-BODY CONFIGURATIONS DESIGNED FOR HIGH LIFT-DRAG RATIOS AT A MACH NUMBER OF 1.4

By Paul G. Fournier

SUMMARY

Tests have been conducted in the Langley high-speed 7- by 10-foot tunnel to investigate the high-subsonic static longitudinal stability characteristics and lift-drag ratios of several wing-body models designed to provide high lift-drag ratios at a Mach number of 1.4. The basic configuration had a thin highly swept wing of aspect ratio 2.91 with NACA 65A-series airfoil sections. Other configurations included bodies modified by two types of indentation and two other wings, one wing without camber but with 4° linear twist (washout) and a second wing with both camber and twist.

The use of wing twist, without camber, provided essentially no improvement in maximum lift-drag ratios over that of the basic flat wing; however, use of a wing having both camber and twist raised the value of maximum lift-drag ratio from 9.0 to 13.5 at a Mach number of 0.60 and from 10.0 to 14.5 at a Mach number of 0.95 for a condition of fixed transition. In general, fixing transition reduced the value of the maximum lift-drag ratio by about 1.5 but had little effect on longitudinal stability. The data show a reduction in static margin with lift coefficient of about 10 percent mean aerodynamic chord at a lift coefficient of 0.2 and, generally, an additional reduction at a lift coefficient of about 0.8.

The present subsonic data show an aerodynamic-center location of approximately 12 percent mean aerodynamic chord ahead of that indicated by unpublished data at a Mach number of 1.41.

INTRODUCTION

This investigation is a part of a continuing investigation being conducted by the National Advisory Committee for Aeronautics to provide data on wing-fuselage configurations designed to have low wave drag and high lift-drag ratios at a Mach number of 1.4. In this series of tests, fuselages having elliptical cross section with body indentations were tested in combination with wings having twisted, cambered, and symmetrical sections.

The purpose of the present investigation is to determine the aerodynamic characteristics of the several wing-fuselage combinations within the subsonic speed range. The Mach number range extended from 0.60 to 0.95 with corresponding Reynolds numbers ranging from 2.0×10^6 to 3.3×10^6 based on the wing mean aerodynamic chord.

SYMBOLS

The data of the present investigation are given about the stability system of axes. The direction of positive forces, moments, and angles are presented in figure 1. All moments of the basic data are referred to the quarter-chord point of the wing mean aerodynamic chord.

C_L	lift coefficient, $\frac{\text{Lift}}{qS}$
C_{L_α}	lift-curve slope, per deg
C_D	drag coefficient, $\frac{\text{Drag}}{qS}$
$C_{D_{C_L=0}}$	drag coefficient at zero lift
C_m	pitching-moment coefficient, $\frac{\text{Pitching moment}}{qS\bar{c}}$
b	wing span, ft
c	wing chord, ft
$\bar{c}$	wing mean aerodynamic chord, ft
t	airfoil thickness, ft

q	free-stream dynamic pressure, $\frac{\rho V^2}{2}$, lb/sq ft
x	distance along X-axis of body from nose, in.
y	distance along Y-axis of body from center line, in.
z	distance along Z-axis of body from center line, in.
A	aspect ratio, b^2/S
L/D	lift-drag ratio
$(L/D)_{max}$	maximum lift-drag ratio
M	Mach number
S	wing area, sq ft
V	free-stream velocity, ft/sec
α	angle of attack, deg
ρ	mass density of air, slugs/cu ft

APPARATUS, MODEL, AND TESTS

Tests were conducted in the Langley high-speed 7- by 10-foot tunnel of a sting-supported wing-fuselage model having an internally mounted electrical strain-gage balance. The model consisted of a combination of any one of three bodies (fuselages) with either a basic flat wing or a twisted wing without camber. (See fig. 2.) Also included was a limited test of a third wing (both twisted and cambered) with one of the bodies. The wings had NACA 65A-series airfoil sections parallel to the plane of symmetry, with thickness-chord ratios t/c of 0.04, 0.035, and 0.03 at the wing root, the 0.5 semispan, and the wing tip, respectively, and had discontinuous sweep and taper. (See fig. 2(a).) The quarter-chord sweep for the inboard section of the wing was 61.71° and was 60° for the outboard section. The wing had an overall taper ratio of 0.167 and an aspect ratio of 2.91. The basic flat wing had no camber or twist. The twisted wing had a linear twist distribution varying from 0° at the wing root to 4° washout at the wing tip. The cambered and twisted wing had an NACA $a = 0$ mean line with a linear variation of camber from 0 percent chord at the wing root to 4 percent chord at the tip, and the same twist as the twisted but uncambered wing.

All fuselages had elliptical cross sections, and the basic fuselage, which was a Sears-Haack body, had an equivalent fineness ratio of 12.5. The other two fuselages were modifications of the basic Sears-Haack body with indentations for $M = 1.4$, one being indented by the area-rule method to approximate the Sears-Haack body distribution and the other being indented by the streamline method to approximate two-dimensional flow at the wing root; these bodies are identified herein as the indented ($M = 1.4$) area-rule body and the indented ($M = 1.4$) streamline body, respectively. The ordinates of the three fuselages are given in table I. Details of the model are given in figure 2. A photograph of the model and support system is shown in figure 3.

Several of the wing-fuselage configurations were tested with transition strips of 0.10-inch width located at 10 percent of the body length and wing chord. The particles used to make up the roughness of the transition strips were No. 120 carborundum, and were selected on the basis of the criteria presented in reference 1.

The model was tested through a Mach number range of 0.60 to 0.95, which corresponds to a Reynolds number range from approximately 2.0×10^6 to 3.3×10^6 based on the wing mean aerodynamic chord. The angle-of-attack range was from -2° to 22°.

CORRECTIONS

Blockage corrections were applied to the data by the method of reference 2. Jet-boundary corrections to angle of attack and drag were applied in accordance with reference 3.

Tares due to the sting support have not been applied, except for a fuselage base-pressure correction to drag since from past experience it has been found that other tares are negligible.

The angles of attack have been corrected for deflection of the sting support and balance under load. No attempt has been made to correct the data for aeroelastic distortion of the steel wing.

RESULTS AND DISCUSSION

The basic longitudinal characteristics for the different model configurations are presented in figures 4 to 9. A summary of some of the more important characteristics is presented in figures 10 to 15.

Longitudinal Stability

The basic static longitudinal results represent a center-of-gravity location at the 0.25$\bar{c}$ location. A comparison of the basic pitching-moment data of figures 4 to 9 and the summary figure 15 shows that there is little difference in the longitudinal stability of the model for any of the wing-fuselage configurations tested, transition free or fixed. There is a difference, however, in the trim pitching-moment coefficient between the basic flat wing and the twisted wing as might be expected for 4° washout at the tip. (See fig. 6.)

The comparison of aerodynamic-center location (fig. 15) for the model configurations show good agreement with that predicted by the theory of reference 4. The pitching-moment curves for all configurations were characterized by a reduction in static margin of about 10 percent mean aerodynamic chord at a lift coefficient of 0.2 and generally an additional reduction at a lift coefficient of about 0.8. A comparison of the subsonic stability data for the wing-body configurations of the present investigation with the supersonic stability data at $M = 1.41$ for the same configuration (unpublished data obtained in the Langley 4- by 4-foot supersonic pressure tunnel) shows that there is approximately a 12-percent mean-aerodynamic-chord rearward shift in aerodynamic-center location from subsonic to supersonic speeds.

Lift

The basic data of figures 4 to 9 show no significant differences in the variation of lift with angle of attack as a result of changing the body indentation, or of fixing transition on the wing and body. The summary of lift-curve slopes C_{L_α} in figure 15 also indicates only minor differences due to configuration changes; in addition, only small increases with Mach number are indicated. Figure 6 shows the effect of twist on lift and indicates, as would be expected from 4° washout at the tip, a small negative increment in lift. Results for the cambered and twisted wing with the indented ($M = 1.4$) area-rule body were obtained only with fixed transition. (See fig. 9.)

Drag

The effects of body indentation on drag at zero lift $C_{D_{C_L=0}}$ were, in general, small and not very consistent (fig. 10). Either type of indentation appeared to reduce the drag at zero lift slightly for the basic flat wing models, but increased the value of $C_{D_{C_L=0}}$ when twist

was used. The Mach number range (0.60 to 0.95) of the present tests is, of course, below that for which substantial benefits due to indentation should be expected.

The effect of fixing transition on the drag at zero lift for the basic flat and the twisted wing with the indented ($M = 1.4$) area-rule body is shown in figure 11. In general, $C_{D_{C_{L=0}}}$ was increased by an increment of about 0.0025 when transition was added, indicating that a substantial amount of laminar flow must have existed for the clean wing. Since there is no outstanding effect of transition on the longitudinal characteristics of a given configuration, the data of figure 9 compared with the data of figure 6 indicate that camber caused a shift in minimum drag to a higher lift coefficient, as might be expected.

Lift-Drag Ratio

The variation of lift-drag ratio with lift coefficient with free and fixed transition for the models with the basic flat wing and the twisted wing with the indented ($M = 1.4$) area-rule body is shown in figure 12. The effect of transition is small at the lower and higher lift coefficients, but in the vicinity of maximum lift-drag ratio there is a decrease in the value of $(L/D)_{max}$ by about 1.5 for the fixed-transition case which is due to the increase in drag at zero lift (fig. 11). Experimental values of the maximum lift-drag ratios for the configuration with the basic flat wing and the indented ($M = 1.4$) area-rule body (free and fixed transition) are compared with theory for full and zero leading-edge suction in figure 13. The results indicate that very little suction was developed, probably because of the high sweep angles and the small leading-edge radii of the airfoil section.

Figure 14 shows the effect of twist and of camber and twist on the variation of maximum lift-drag ratios with Mach number. The data at $M = 1.41$ (unpublished data) show that twist provided a small increment in $(L/D)_{max}$ but camber seemed to give no additional advantage (actually a small decrease). The data at the present test Mach numbers, however, showed that the effect of camber was very beneficial (increased $(L/D)_{max}$ from 9.0 to 13.5 at $M = 0.60$ and from 10.0 to 14.5 at $M = 0.95$), and the effect of twist was negligible. It should be kept in mind that the data at $M = 0.60$ to 0.95 had fixed transition, whereas the data at $M = 1.41$ had free transition; this, however, should only affect the profile drag which would in effect be approximately the same for all wings because of the location of the transition strips.

CONCLUSIONS

The results of a subsonic static longitudinal stability investigation conducted in the Langley high-speed 7- by 10-foot tunnel of several wing-body configurations designed for high lift-drag ratios at a Mach number of 1.4 indicate the following conclusions:

1. The use of wing twist, without camber, provided essentially no improvement in maximum lift-drag ratios over that of the basic flat wing; however, use of a wing having both camber and twist raised the value of maximum lift-drag ratio from 9.0 to 13.5 at a Mach number of 0.60 and from 10.0 to 14.5 at a Mach number of 0.95 for a condition of fixed transition.

2. In general, fixing transition reduced the value of maximum lift-drag ratio by about 1.5 for the test conditions, but had little effect on longitudinal stability.

3. Body indentation has essentially no effect on either longitudinal stability characteristics or maximum lift-drag ratios within the Mach number range investigated. The pitching-moment curves for all configurations were characterized by a reduction in static margin of about 10 percent mean aerodynamic chord at a lift coefficient of 0.2 and, generally, an additional reduction at a lift coefficient of about 0.8.

4. The static margin could be predicted with reasonable accuracy by means of the available theory. Supersonic data at a Mach number of 1.41 indicate a rearward shift in aerodynamic-center location of approximately 12 percent mean aerodynamic chord over that of data at subsonic speeds.

Langley Aeronautical Laboratory,
National Advisory Committee for Aeronautics,
Langley Field, Va., March 18, 1958.

REFERENCES

1. Von Doenhoff, Albert E., and Horton, Elmer A.: A Low-Speed Experimental Investigation of the Effect of a Sandpaper Type of Roughness on Boundary-Layer Transition. NACA Rep. 1349, 1958. (Supersedes NACA TN 3858.)

2. Herriot, John G.: Blockage Corrections for Three-Dimensional-Flow Closed-Throat Wind Tunnels, With Consideration of the Effect of Compressibility. NACA Rep. 995, 1950. (Supersedes NACA RM A7B28.)

3. Gillis, Clarence L., Polhamus, Edward C., and Gray, Joseph L., Jr.: Charts for Determining Jet-Boundary Corrections for Complete Models in 7- by 10-Foot Closed Rectangular Wind Tunnels. NACA WR L-123, 1945. (Formerly NACA ARR L5G31.)

4. McLaughlin, Milton D.: Method of Estimating the Stick-Fixed Longitudinal Stability of Wing-Fuselage Configurations Having Unswept or Swept Wings. NACA RM L51J23, 1952.

TABLE I.- BODY ORDINATES

[All dimensions in inches]

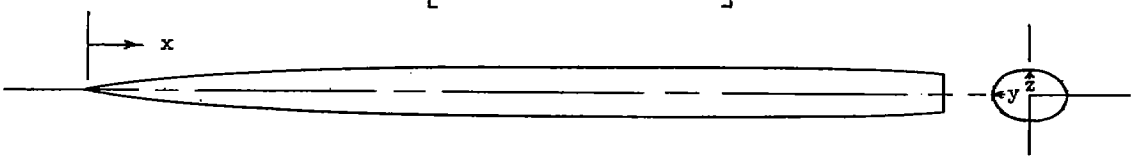

x	z for all bodies	y for -		
		Basic body	Indented (M = 1.4) area-rule body	Indented (M = 1.4) streamline body
0	0	0	0	0
1	.198	.297	.297	.297
2	.328	.492	.492	.492
3	.437	.655	.655	.655
4	.533	.799	.799	.799
5	.619	.928	.928	.928
6	.696	1.045	1.045	1.045
7	.767	1.151	1.151	1.151
8	.832	1.248	1.248	1.248
9	.891	1.337	1.337	1.337
10	.945	1.418	1.418	1.418
11	.995	1.492	1.492	1.492
12	1.040	1.559	1.559	1.559
13	1.080	1.620	1.620	1.620
14	1.116	1.670	1.666	1.675
15	1.149	1.720	1.666	1.699
16	1.175	1.765	1.645	1.690
17	1.190	1.800	1.609	1.656
18	1.195	1.835	1.551	1.610
19	↓	1.860	1.482	1.558
20		1.880	1.399	1.497
21		1.895	1.325	1.437
22		1.906	1.257	1.381
23		1.910	1.198	1.327
24		1.910	1.211	1.281
25		1.905	1.260	1.243
26		1.894	1.332	1.215
27		1.879	1.446	1.198
28		1.856	1.514	1.197
29		1.824	1.542	1.210
30		1.796	1.554	1.232
31		1.758	1.534	1.249
32		1.714	1.489	1.255
33		1.665	1.433	1.240
34	1.182	1.610	1.369	1.210
35	1.155	1.550	1.303	1.170
36	1.117	1.478	1.231	1.125
37	1.072	1.365	1.155	1.077
38	1.025	1.226	1.067	1.027
39	.975	.975	.975	.975

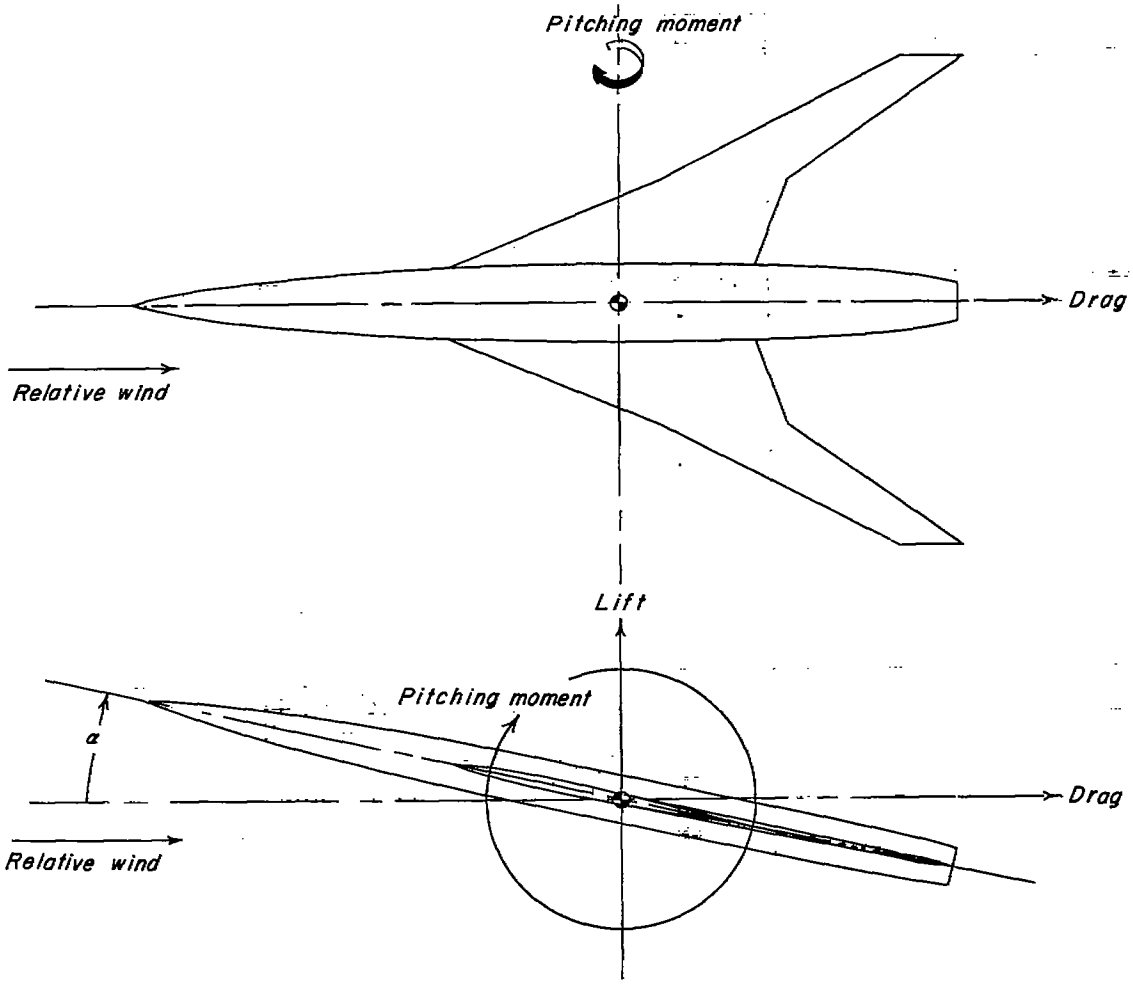

Figure 1.- Stability system of axes showing positive direction of forces, moment, and angle.

Wing

	L.E.	T.E.
Sweep		
Inboard	67.01°	19.65°
Outboard	61.70°	53.61°
Area, sq ft		1.375
Aspect ratio		2.91
Taper ratio		.167
Mean aerodynamic chord, ft		.895
Airfoil section parallel to plane of symmetry		
root		65A004
.5 semispan		65A0035
tip		65A003

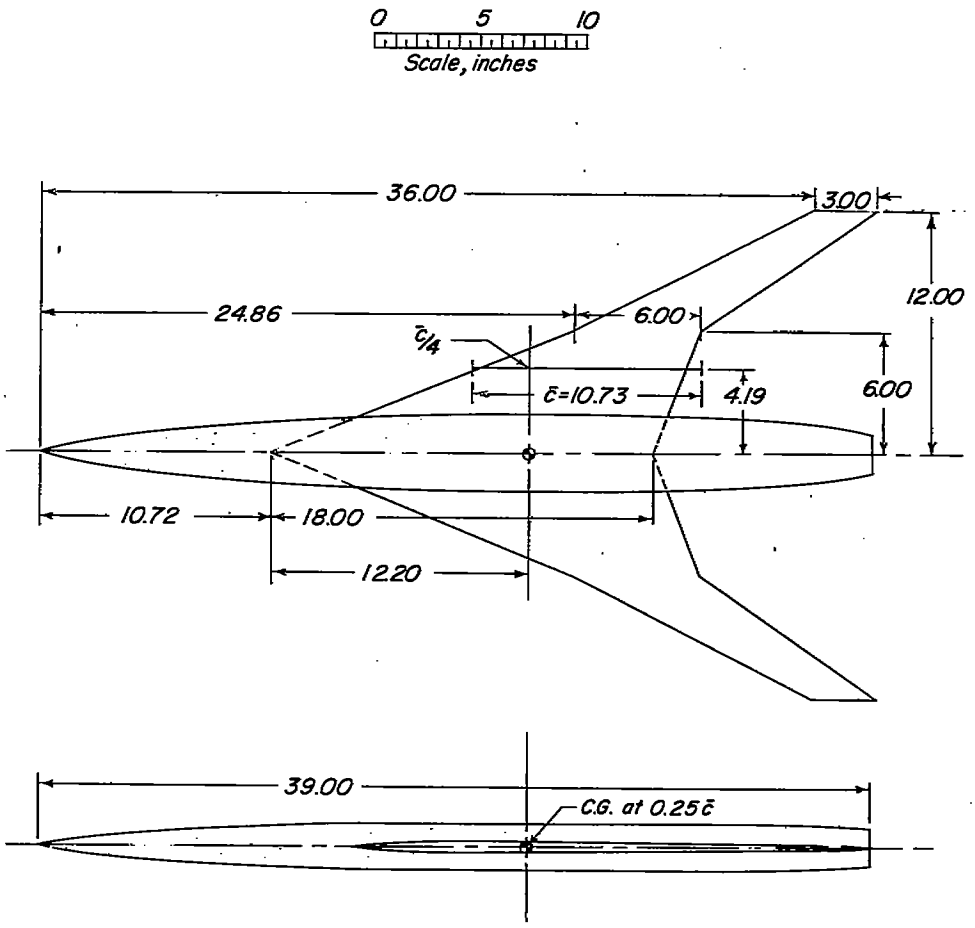

(a) Model.

Figure 2.- Details of model. (All dimensions in inches.)

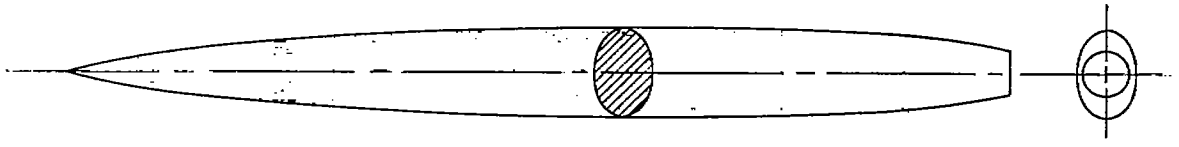

Basic Sears-Haack body

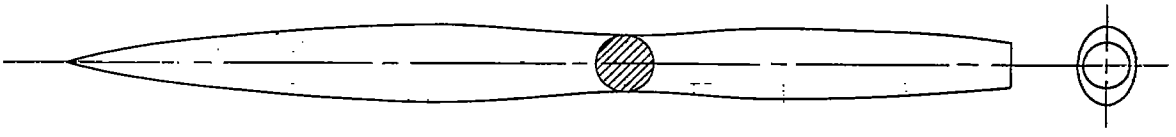

Indented (M=1.4) area-rule body

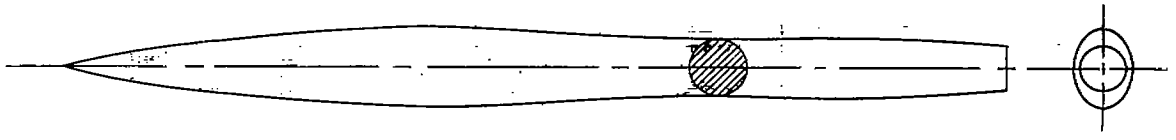

Indented (M=1.4) streamline body

Plan views

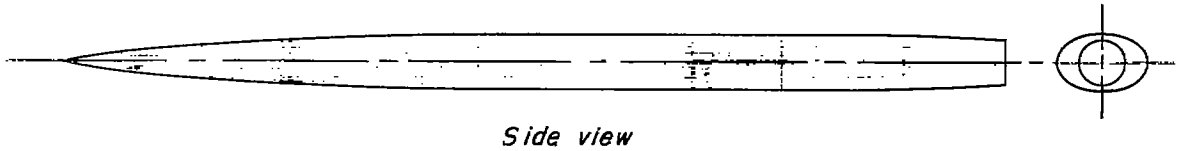

Side view

(b) Bodies.

Figure 2.- Concluded.

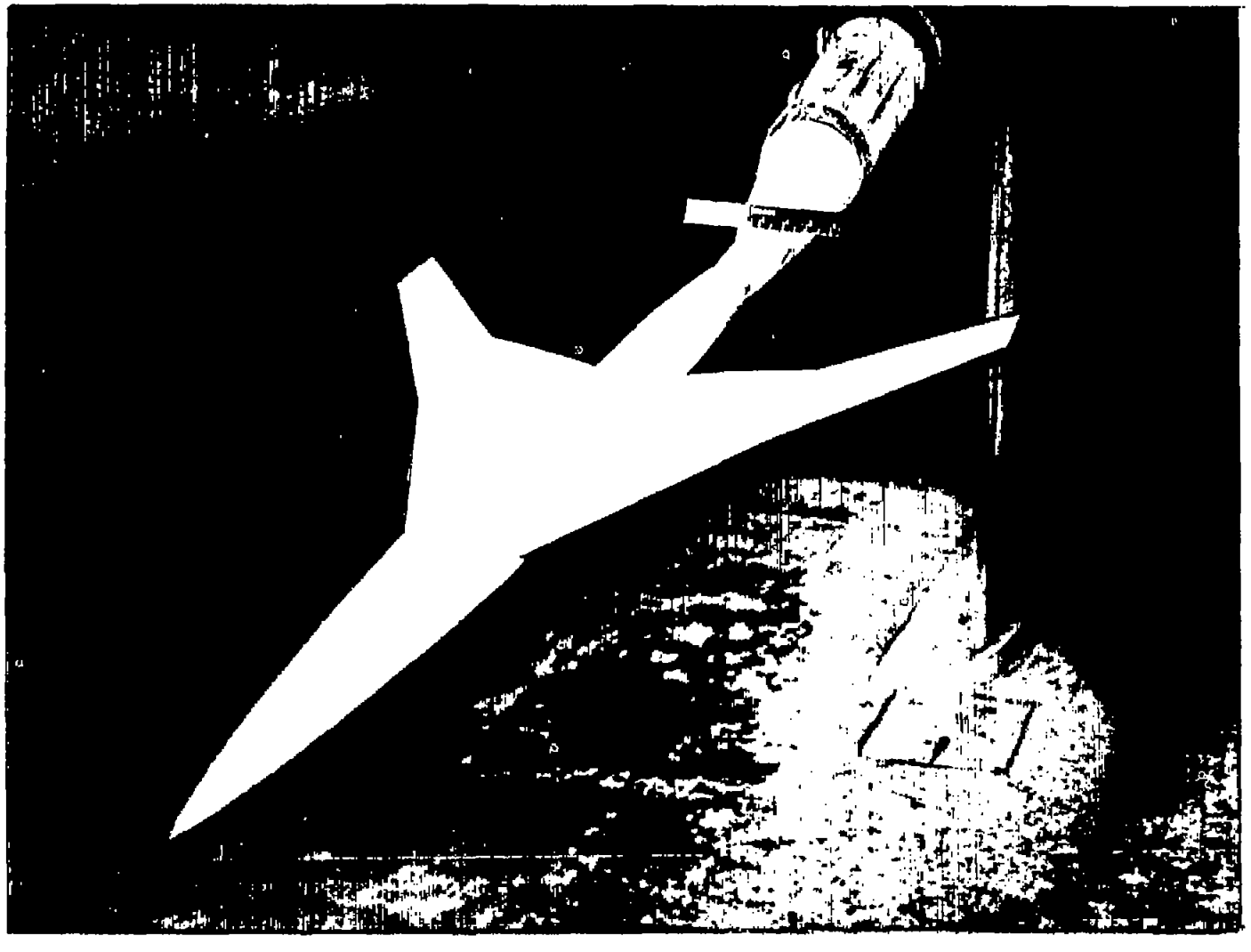

L-57-2046

Figure 3.- Photograph of typical model, including the sting support.

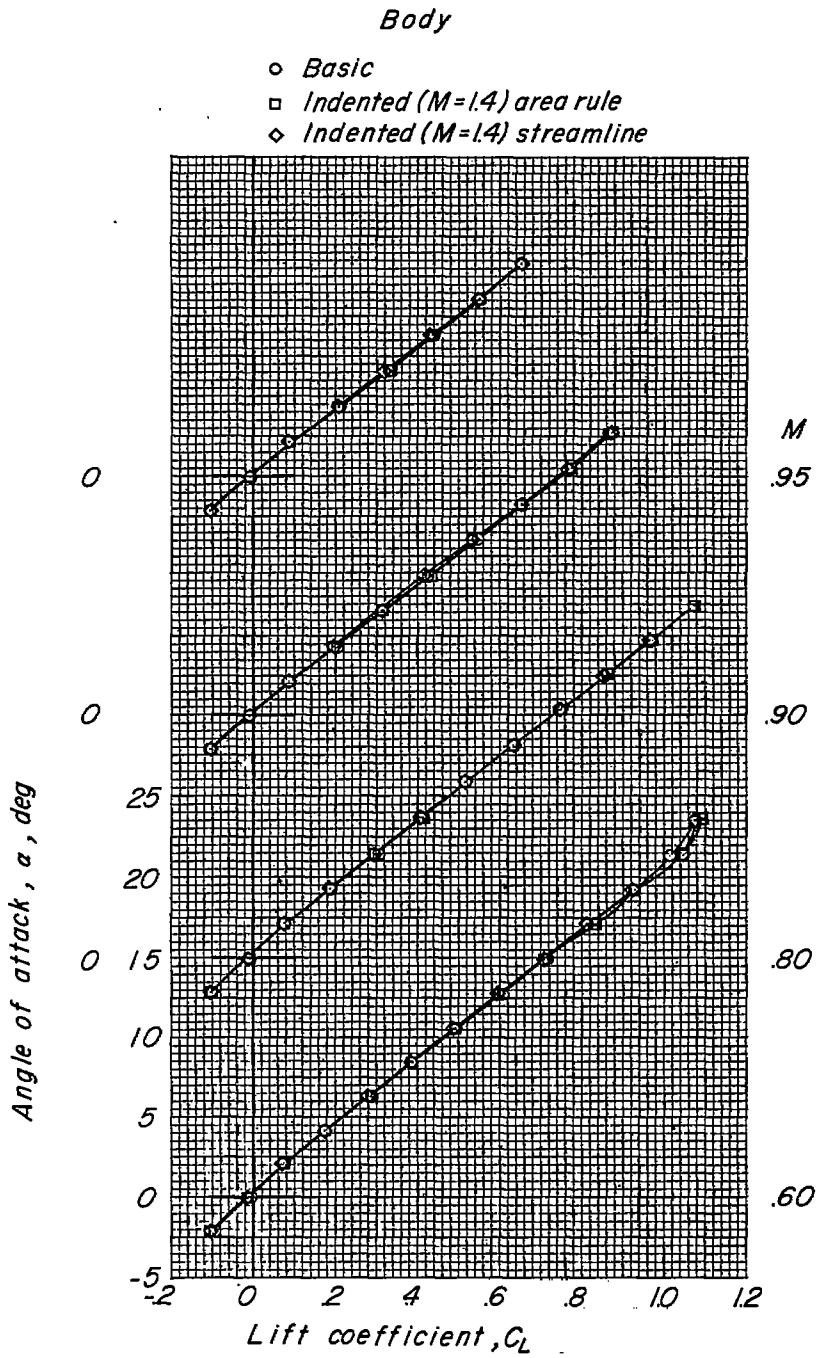

(a) Variation of α with C_L.

Figure 4.- Longitudinal characteristics of wing-fuselage model with basic flat wing. Free transition.

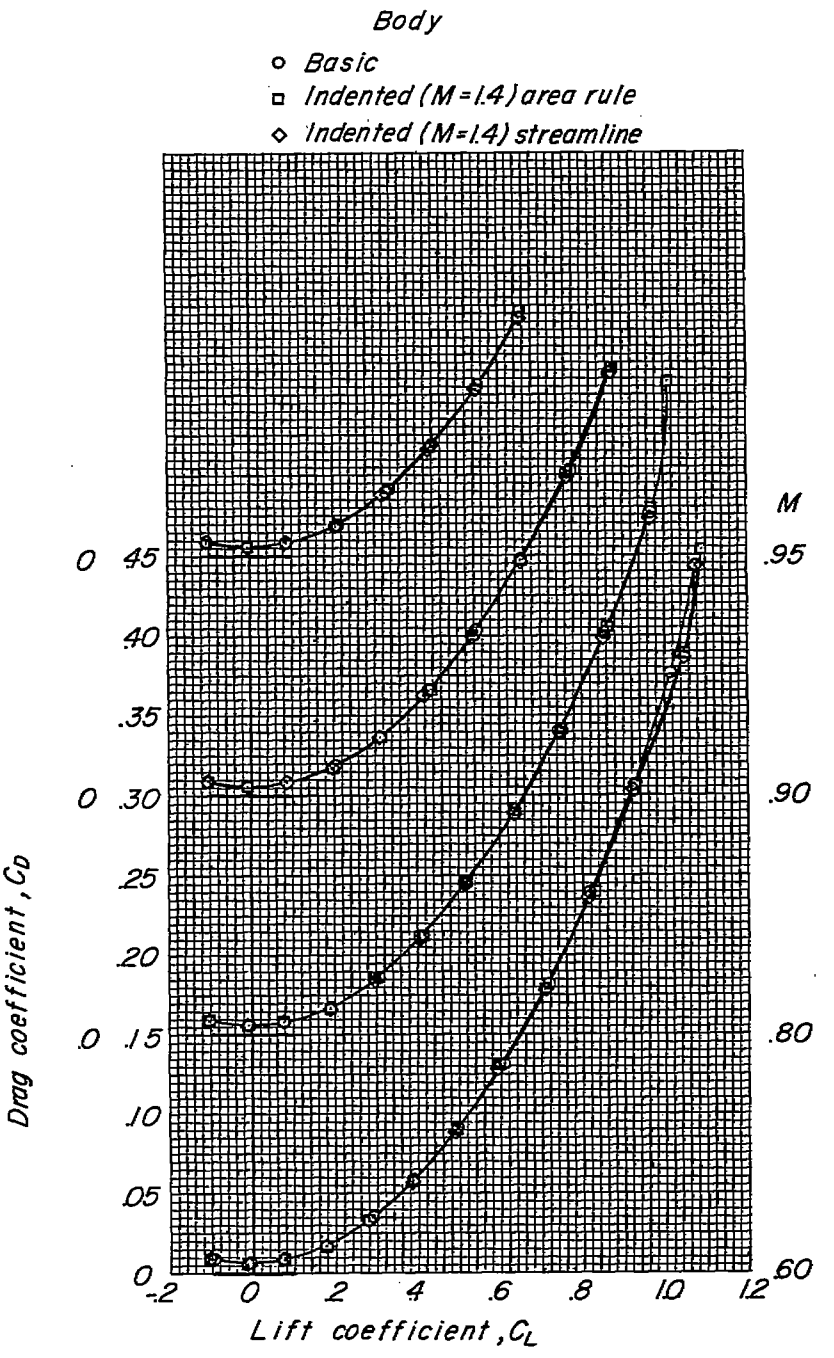

(b) Variation of C_D with C_L.

Figure 4.- Continued.

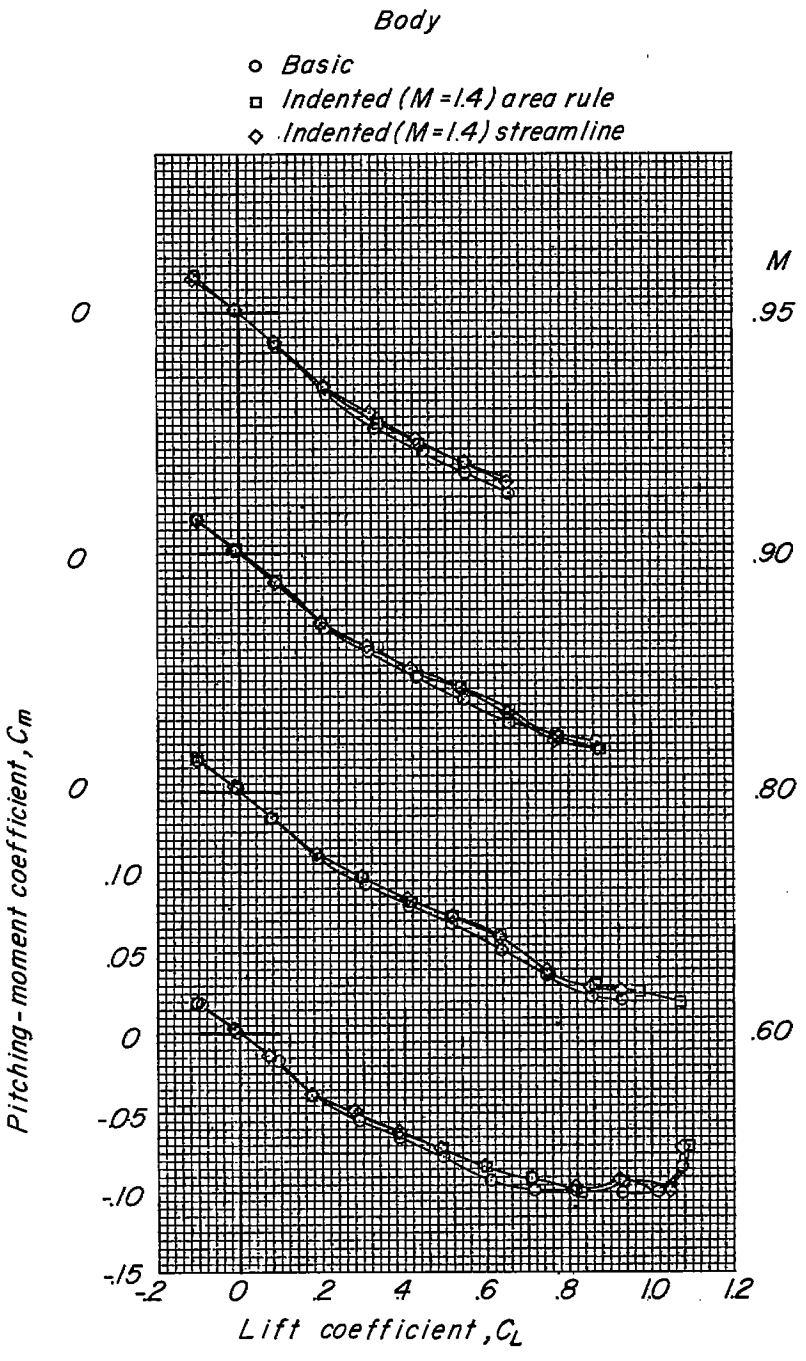

(c) Variation of C_m with C_L.

Figure 4.- Continued.

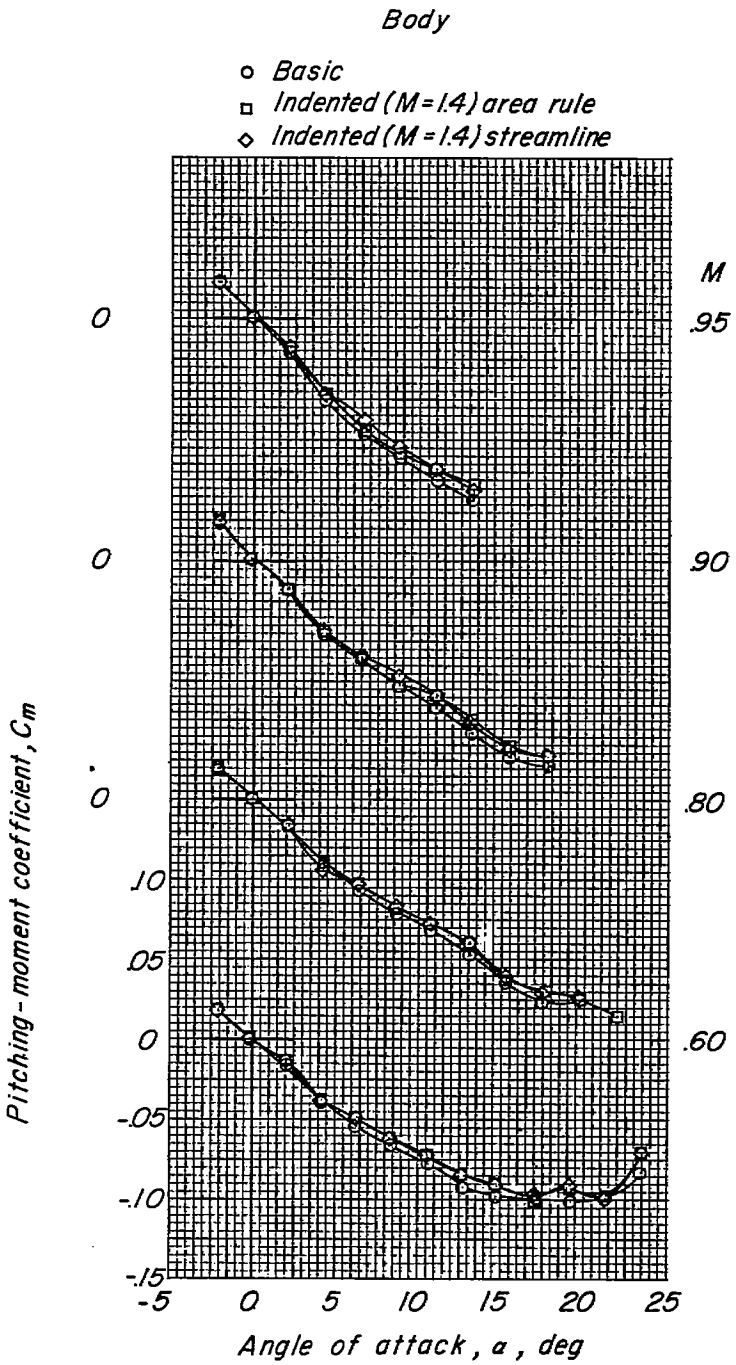

(d) Variation of C_m with α.

Figure 4.- Concluded.

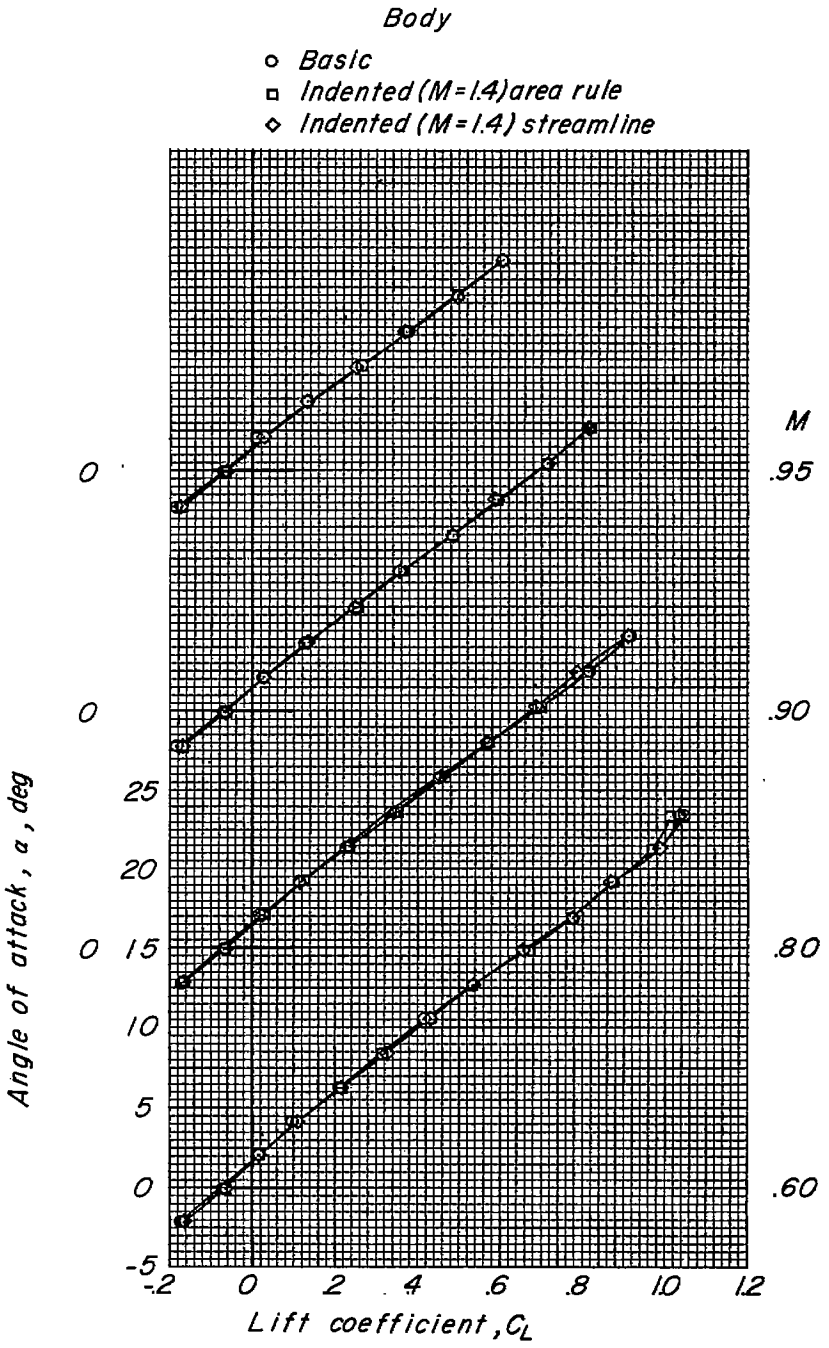

(a) Variation of α with C_L.

Figure 5.- Longitudinal characteristics of wing-fuselage model with twisted wing. Free transition.

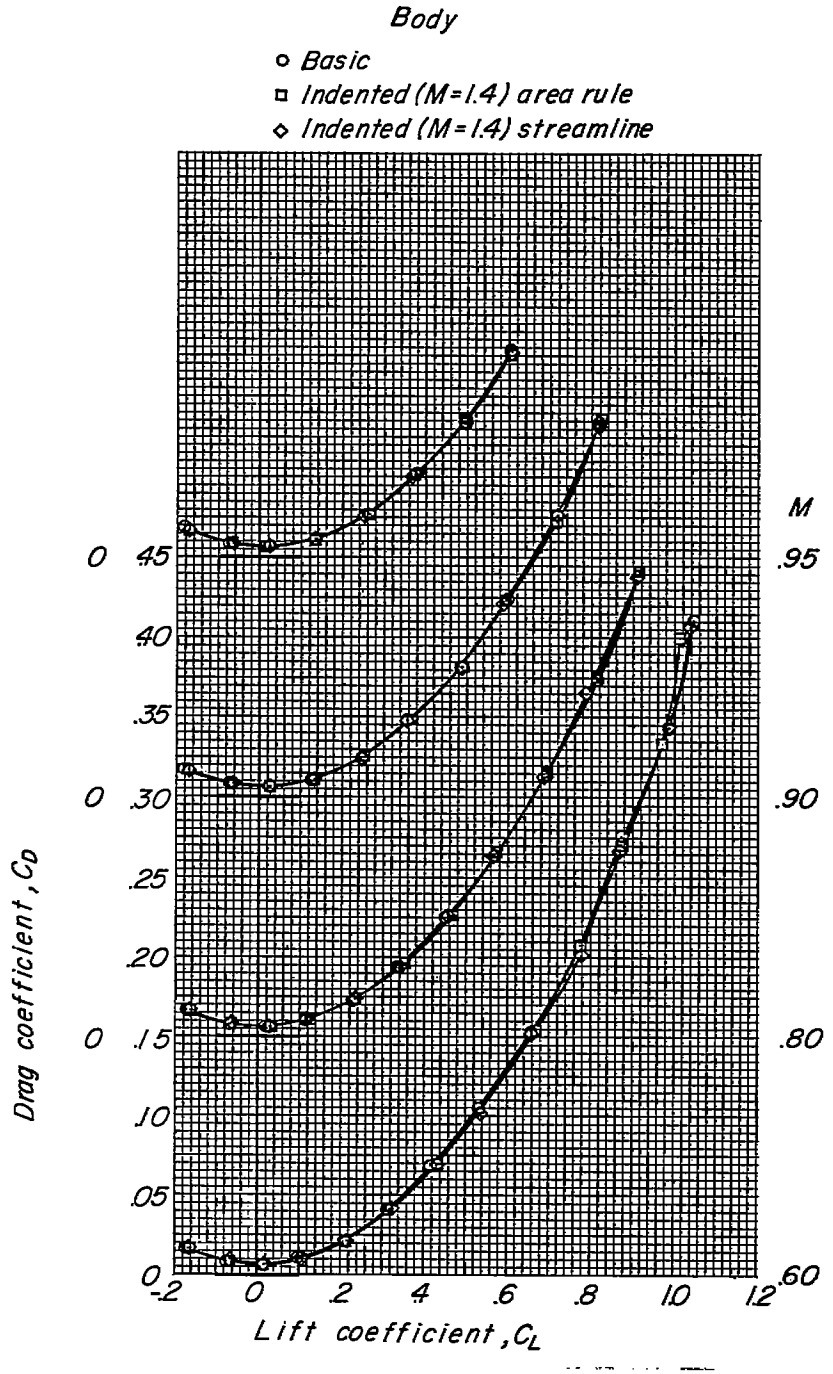

(b) Variation of C_D with C_L.

Figure 5.- Continued.

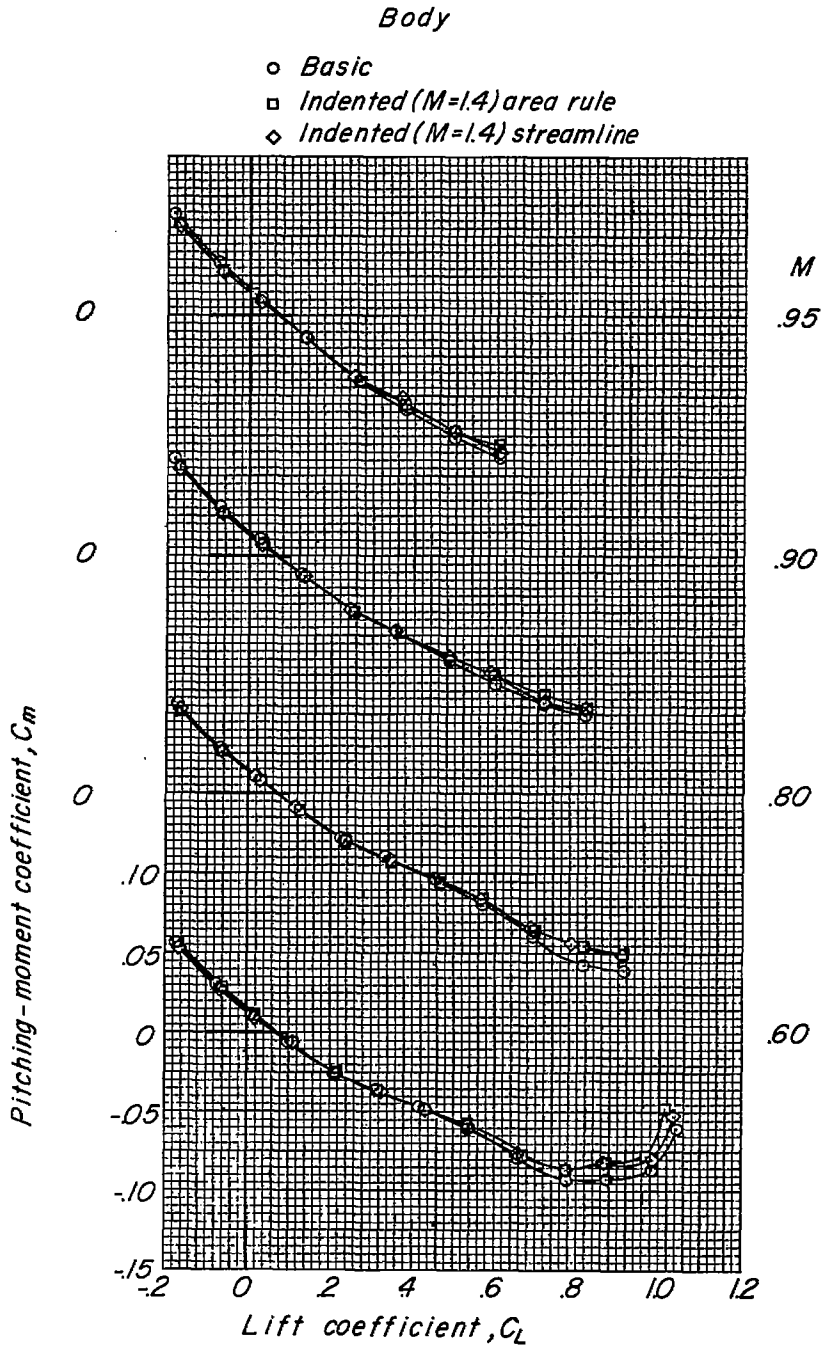

(c) Variation of C_m with C_L.

Figure 5.- Continued.

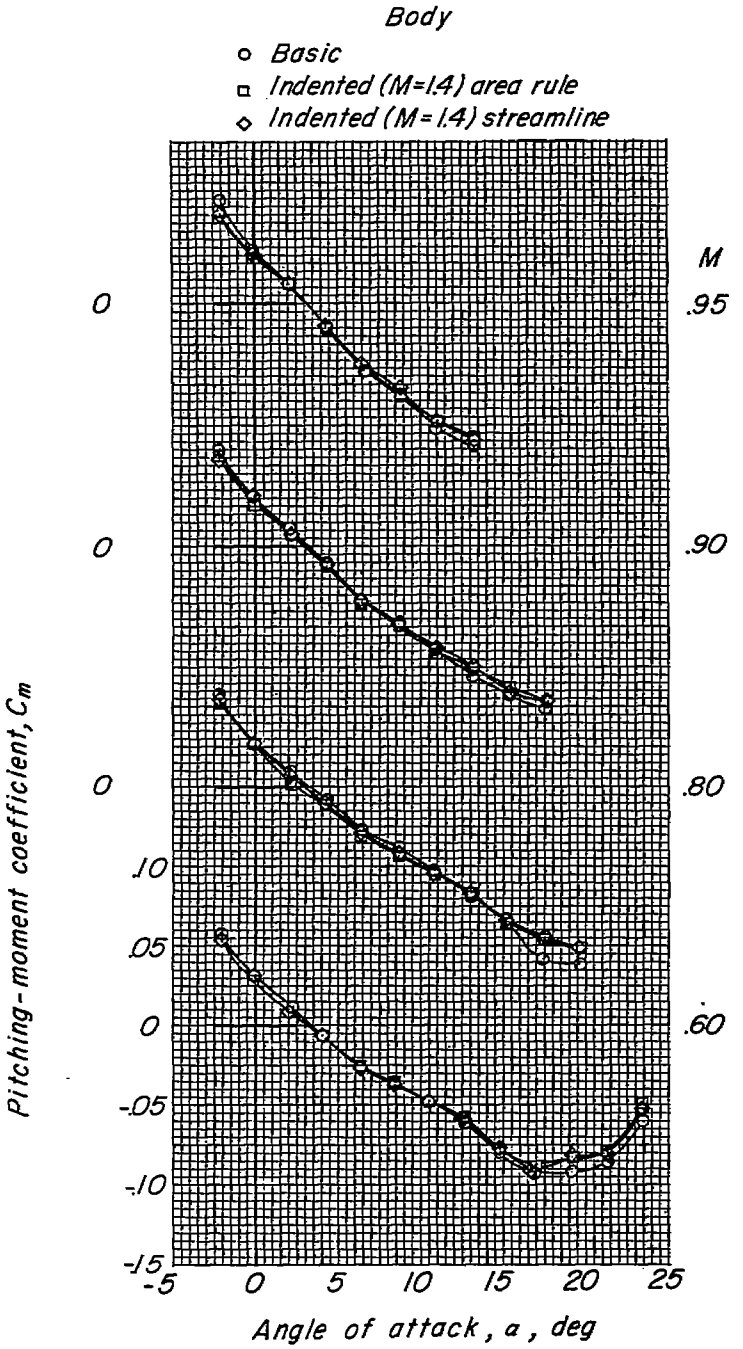

(d) Variation of C_m with α.

Figure 5.- Concluded.

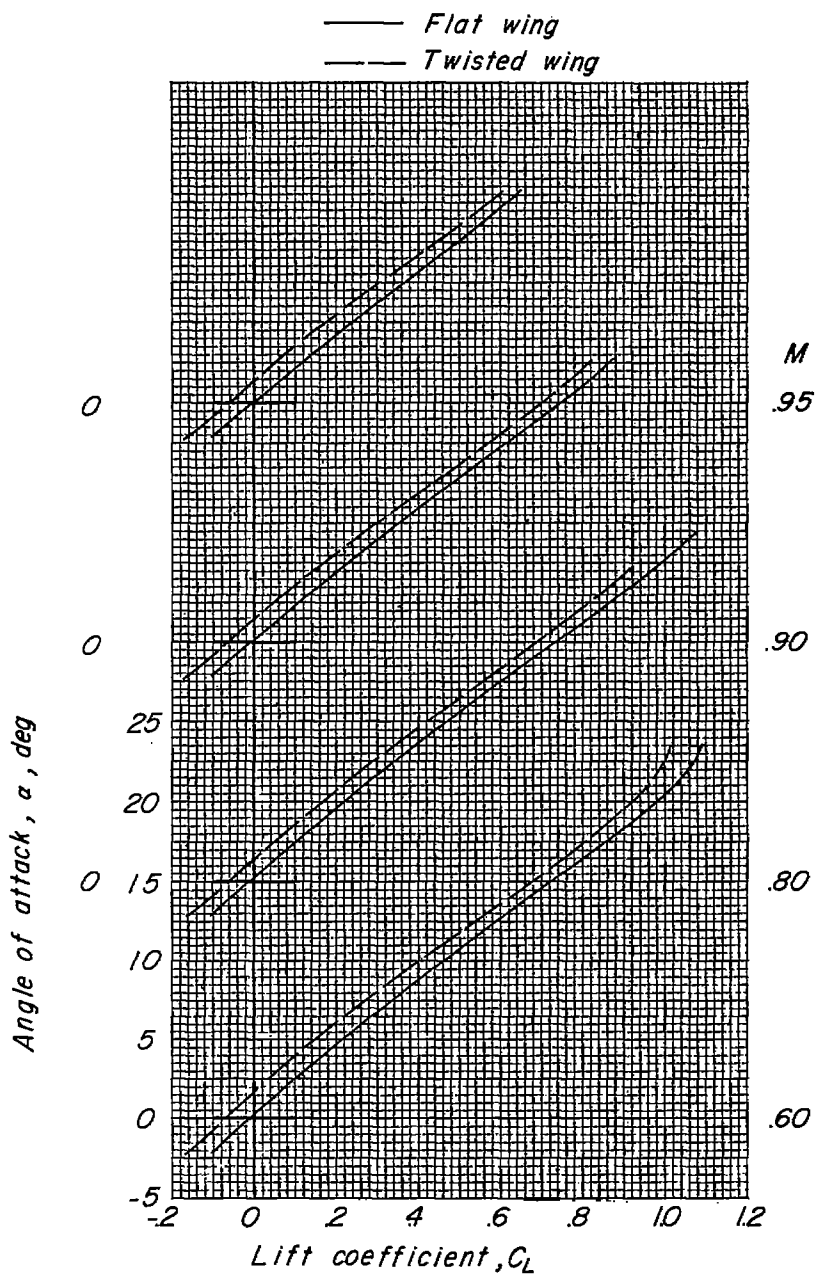

(a) Variation of α with C_L.

Figure 6.- Effect of twist on the longitudinal characteristics of wing-fuselage model with indented (M = 1.4) area-rule body. Free transition.

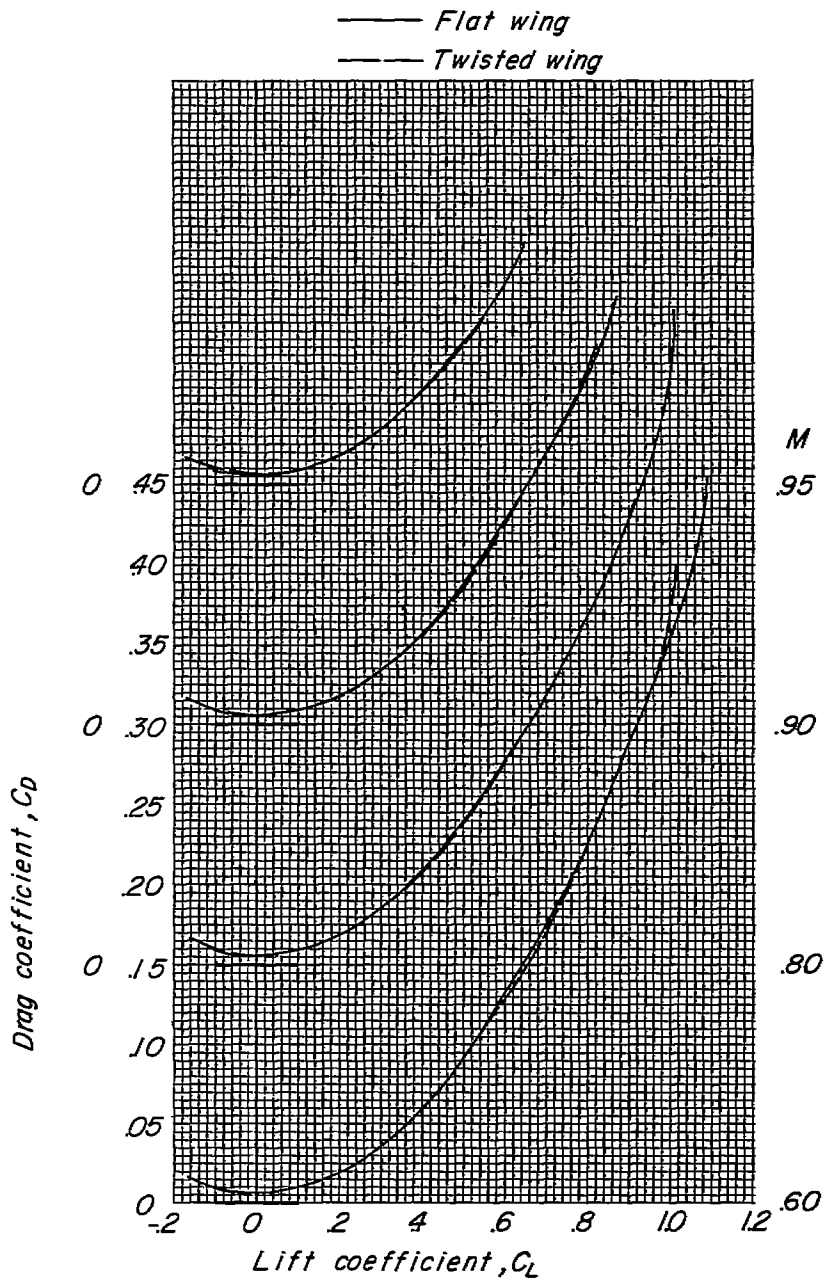

(b) Variation of C_D with C_L.

Figure 6.- Continued.

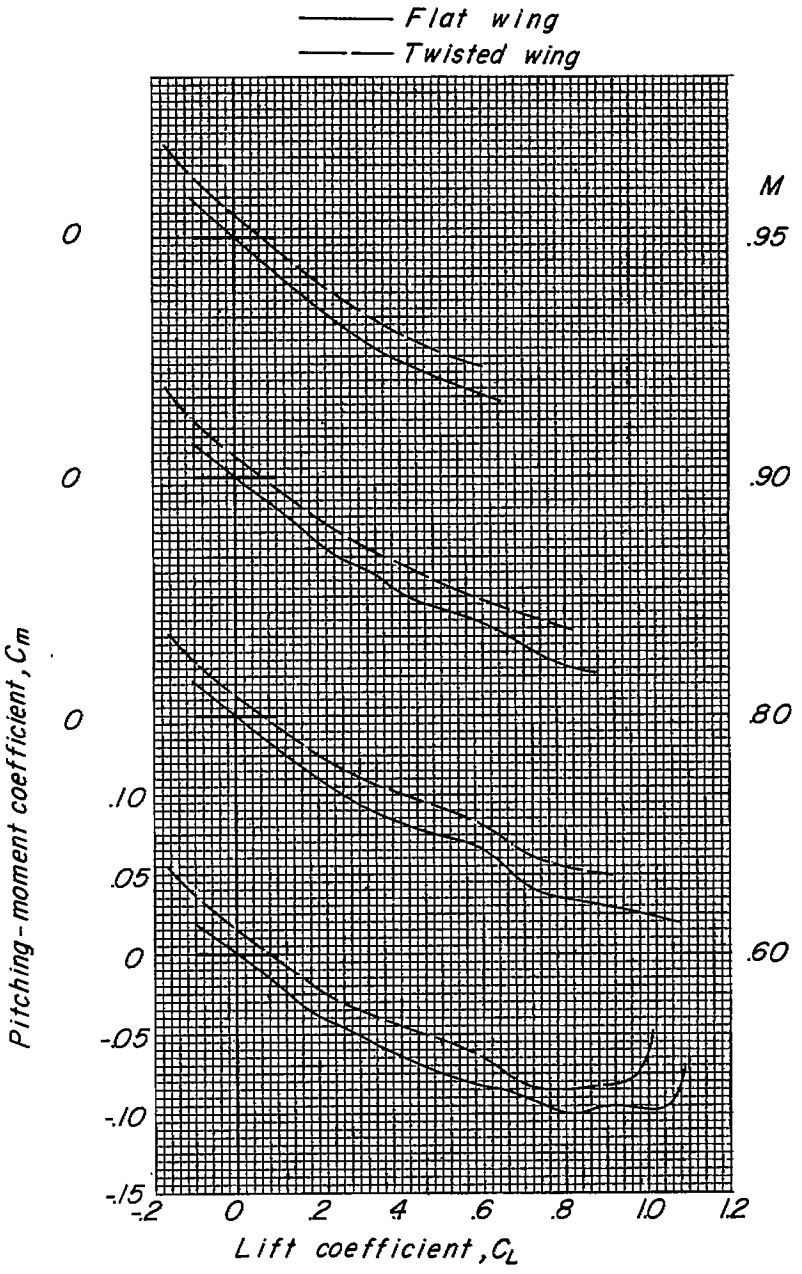

(c) Variation of C_m with C_L.

Figure 6.- Continued.

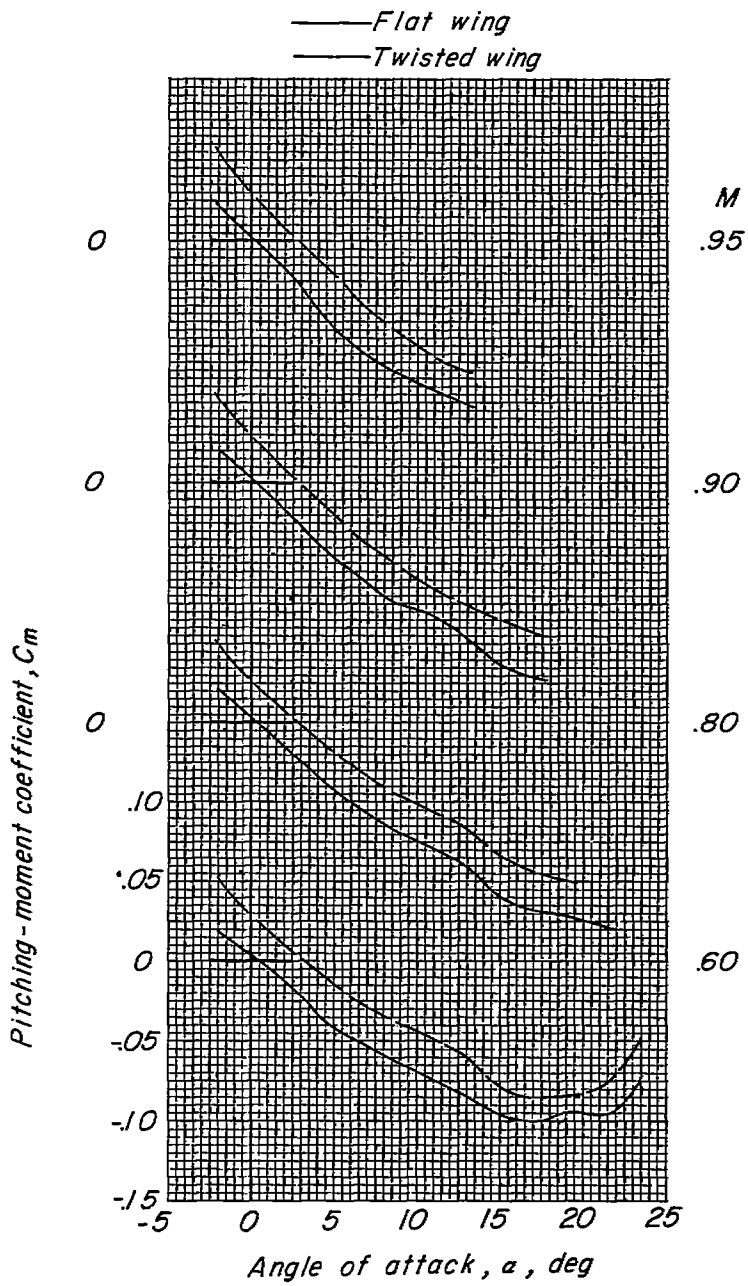

(d) Variation of C_m with α.

Figure 6.- Concluded.

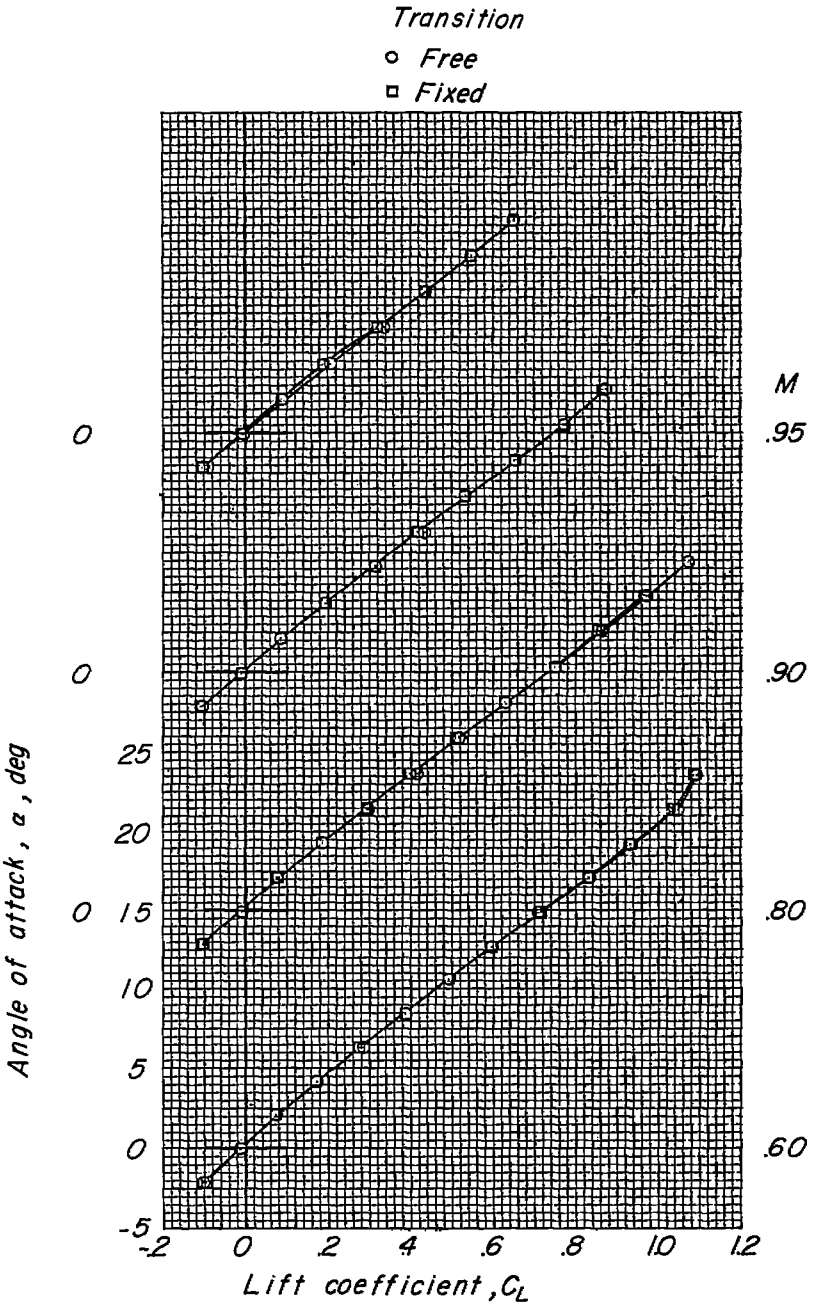

(a) Variation of α with C_L.

Figure 7.- Longitudinal characteristics of wing-fuselage model with basic flat wing and indented (M = 1.4) area-rule body.

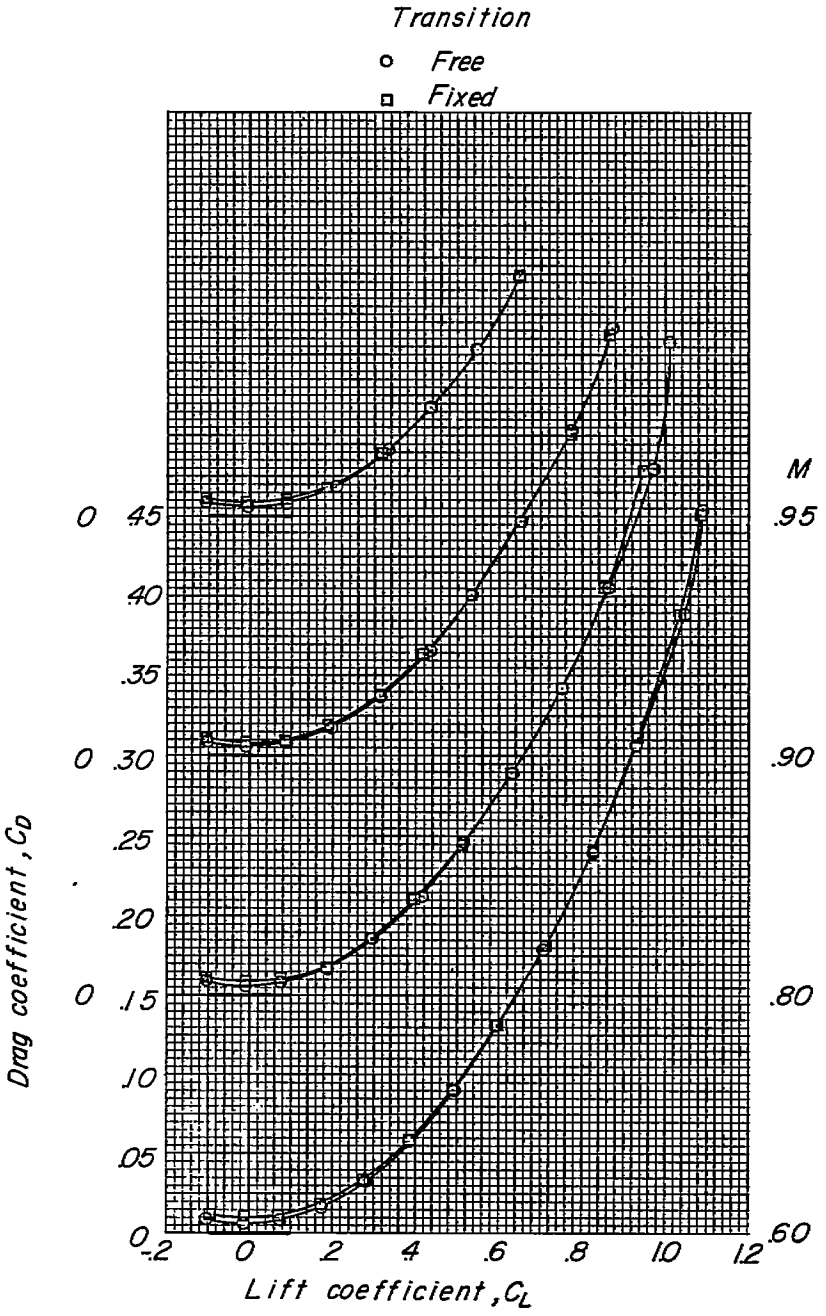

(b) Variation of C_D with C_L.

Figure 7.- Continued.

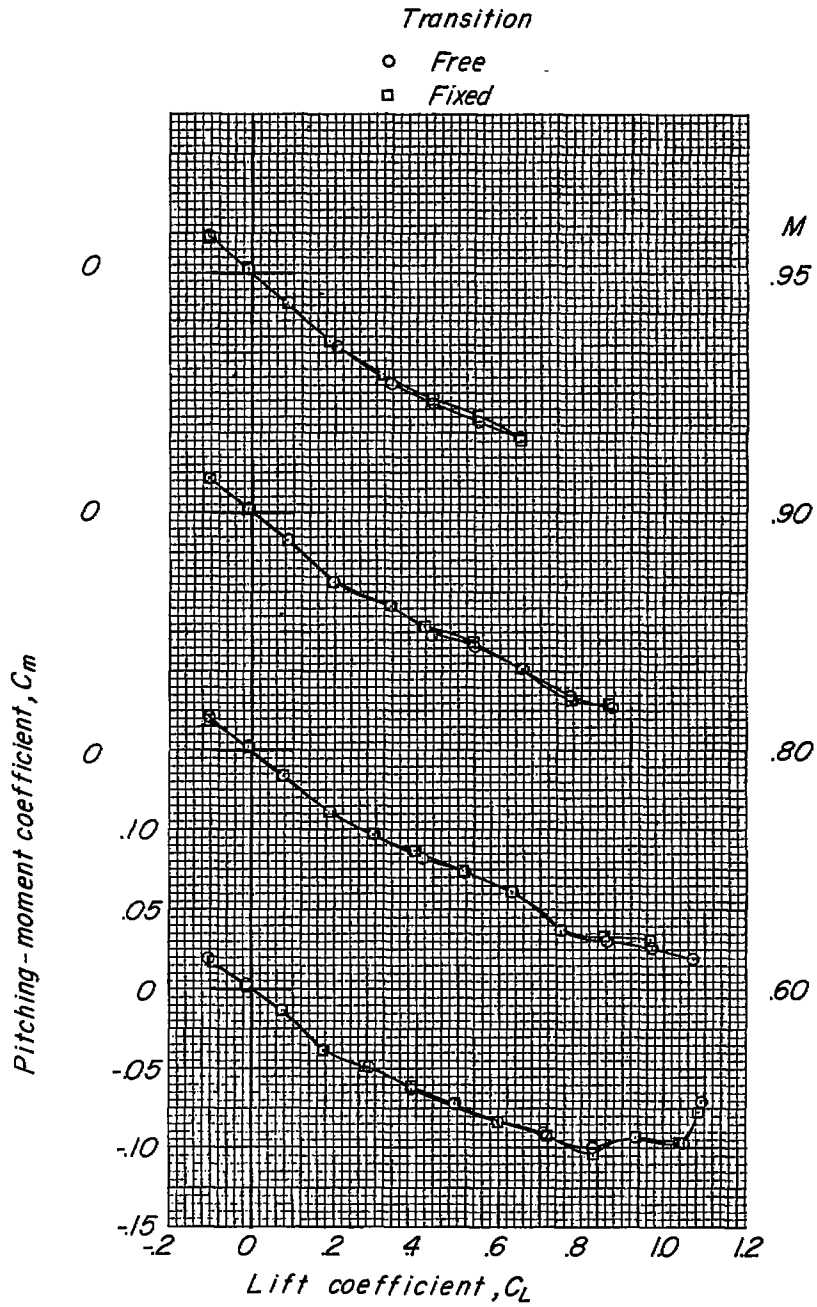

(c) Variation of C_m with C_L.

Figure 7.- Continued.

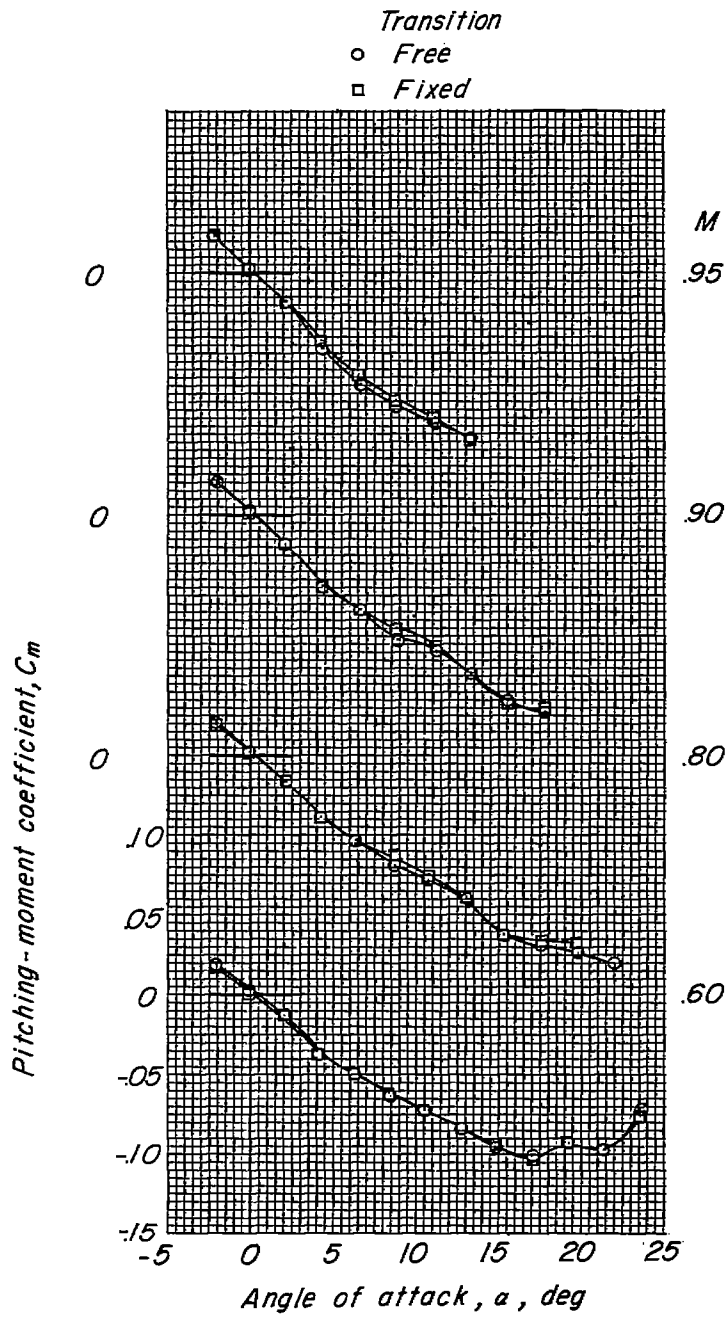

(d) Variation of C_m with α.

Figure 7.- Concluded.

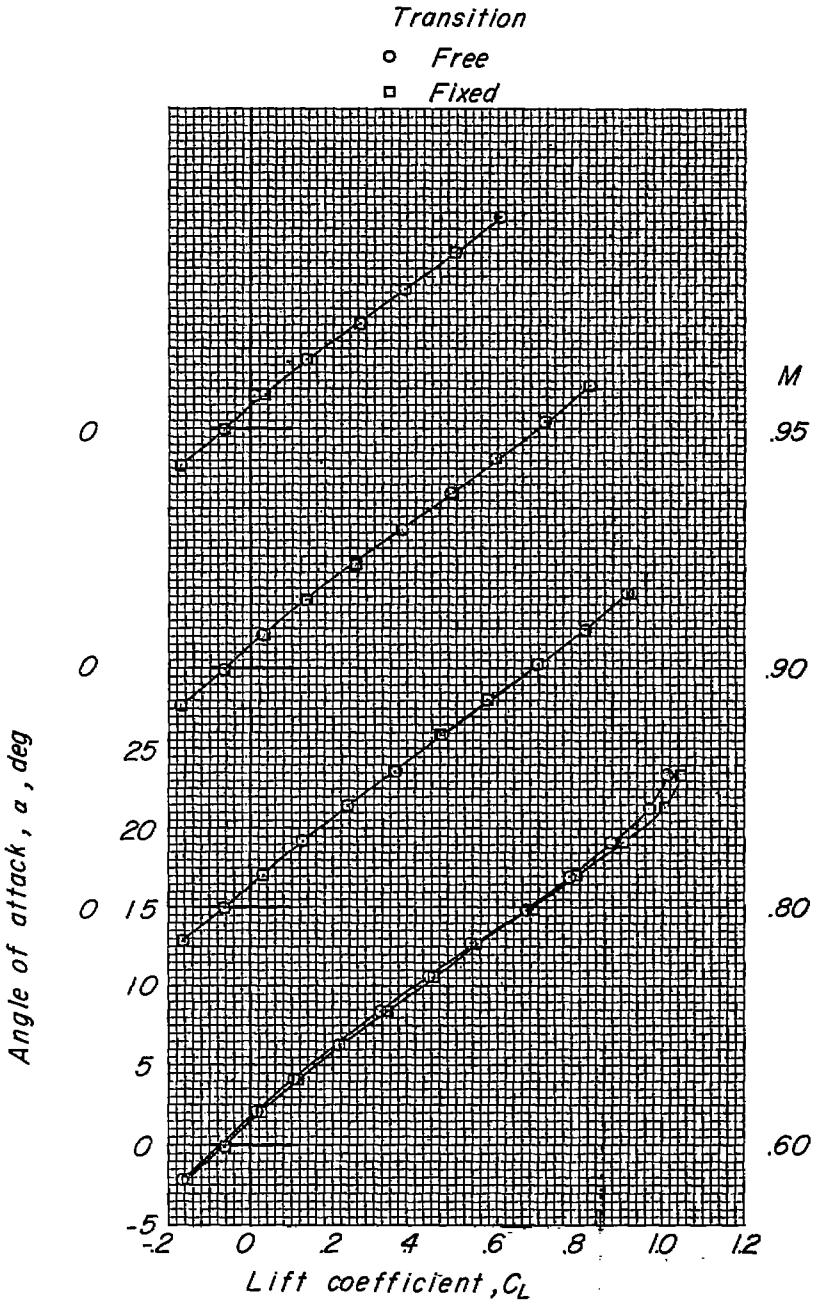

(a) Variation of α with C_L.

Figure 8.- Longitudinal characteristics of wing-fuselage model with twisted wing and indented (M = 1.4) area-rule body.

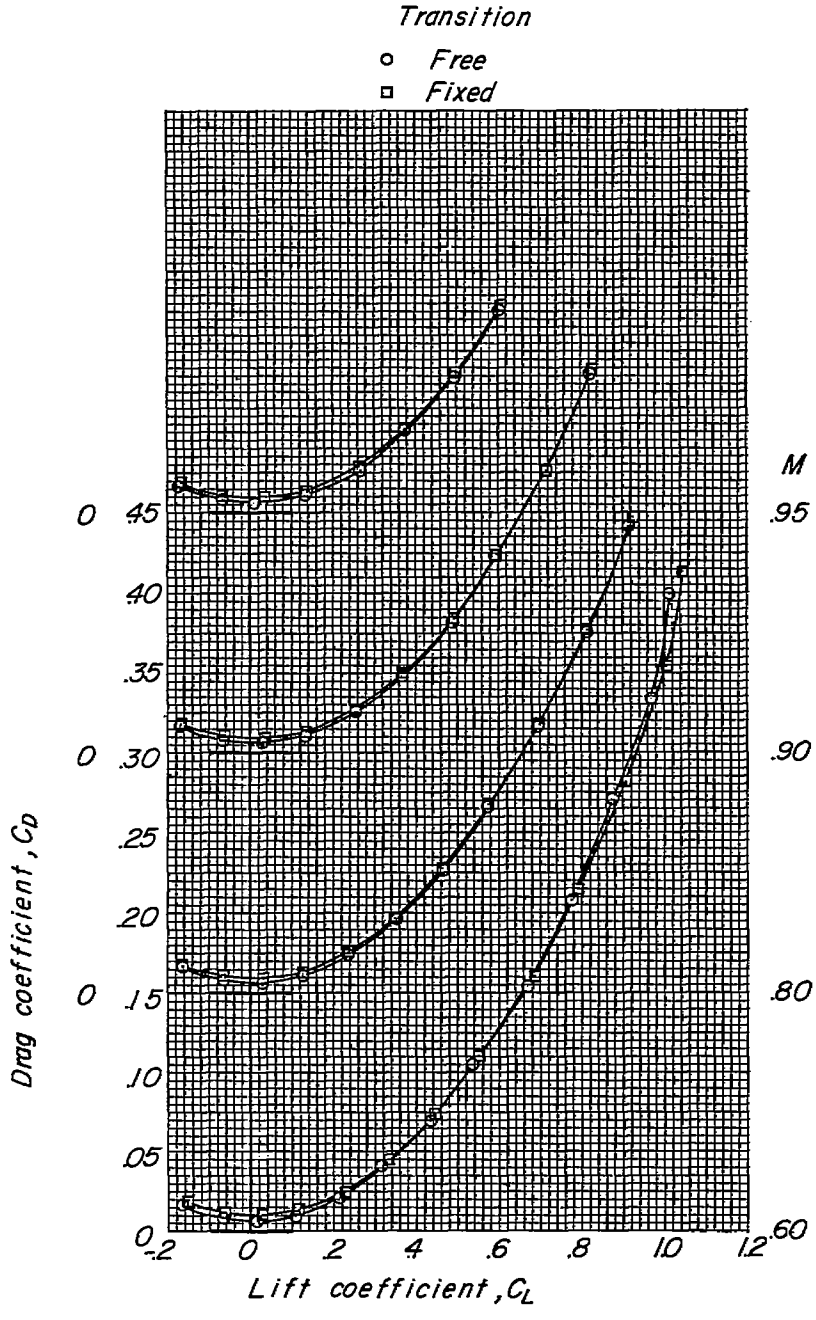

(b) Variation of C_D with C_L.

Figure 8.- Continued.

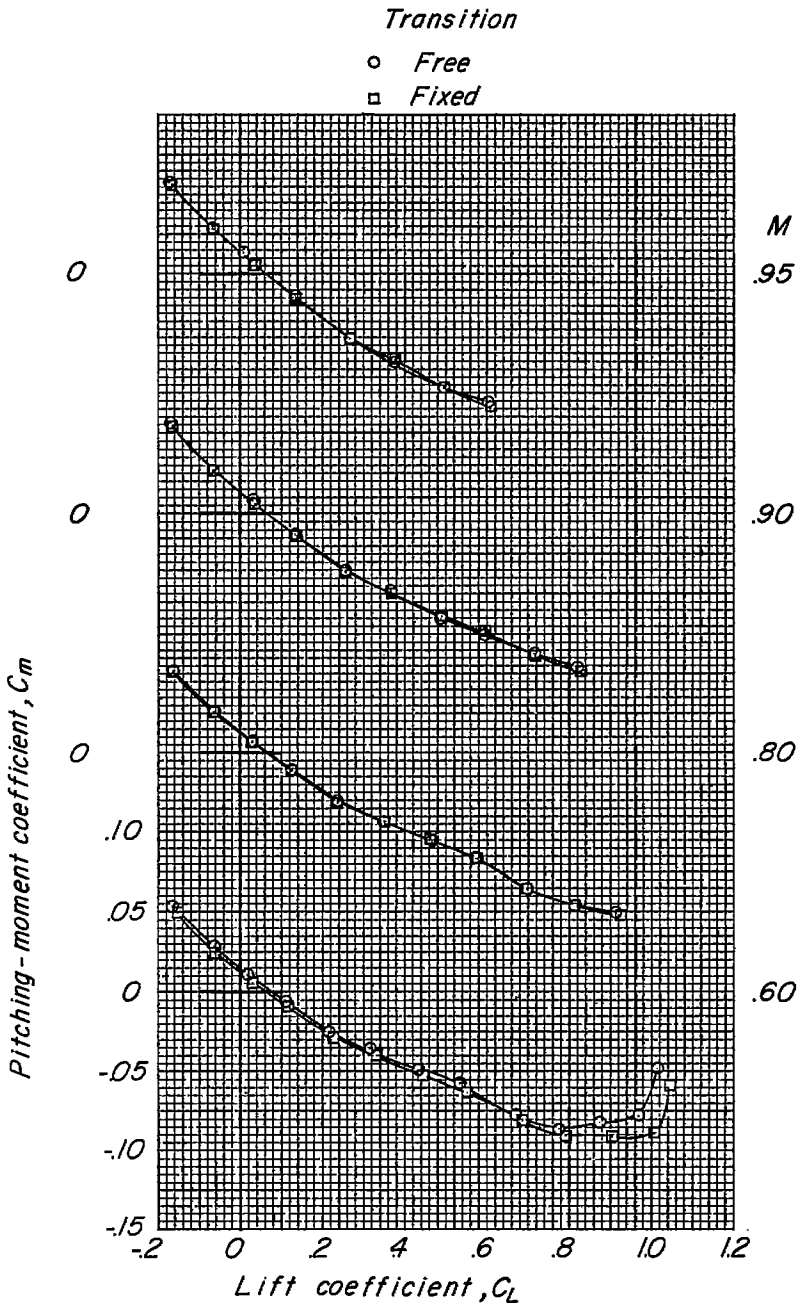

(c) Variation of C_m with C_L.

Figure 8.- Continued.

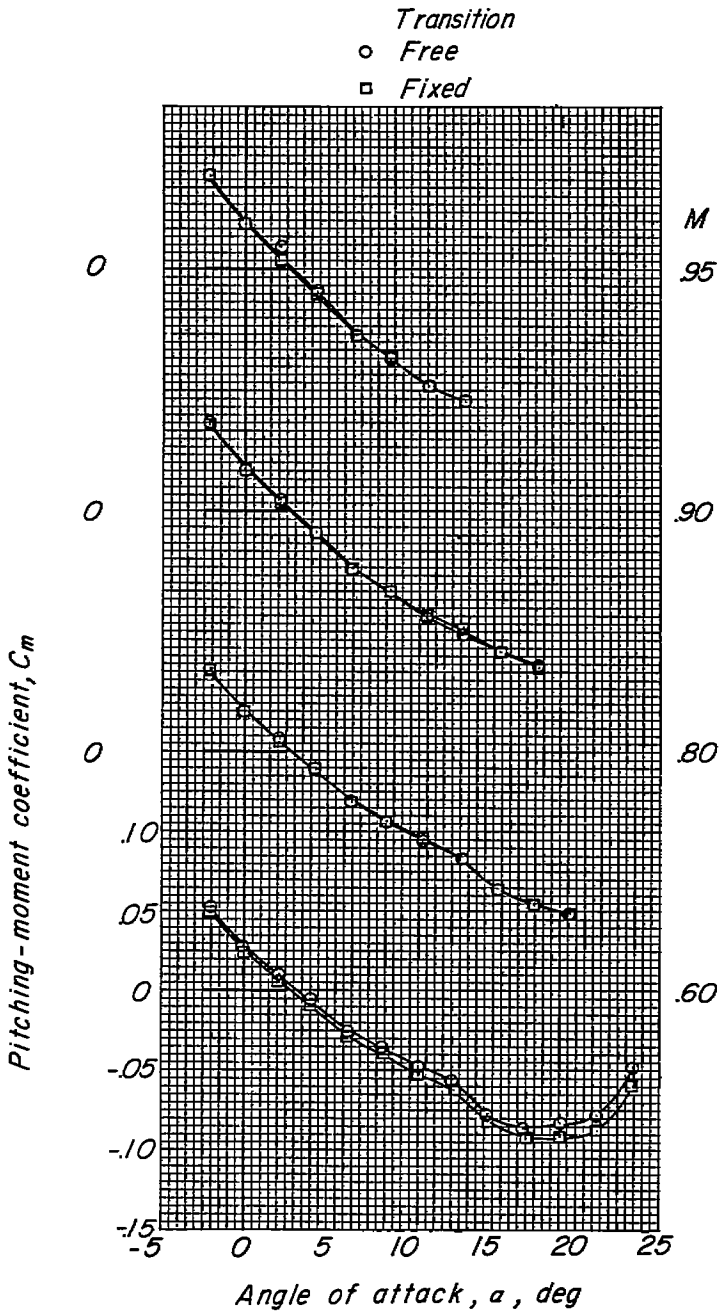

(d) Variation of C_m with α.

Figure 8.- Concluded.

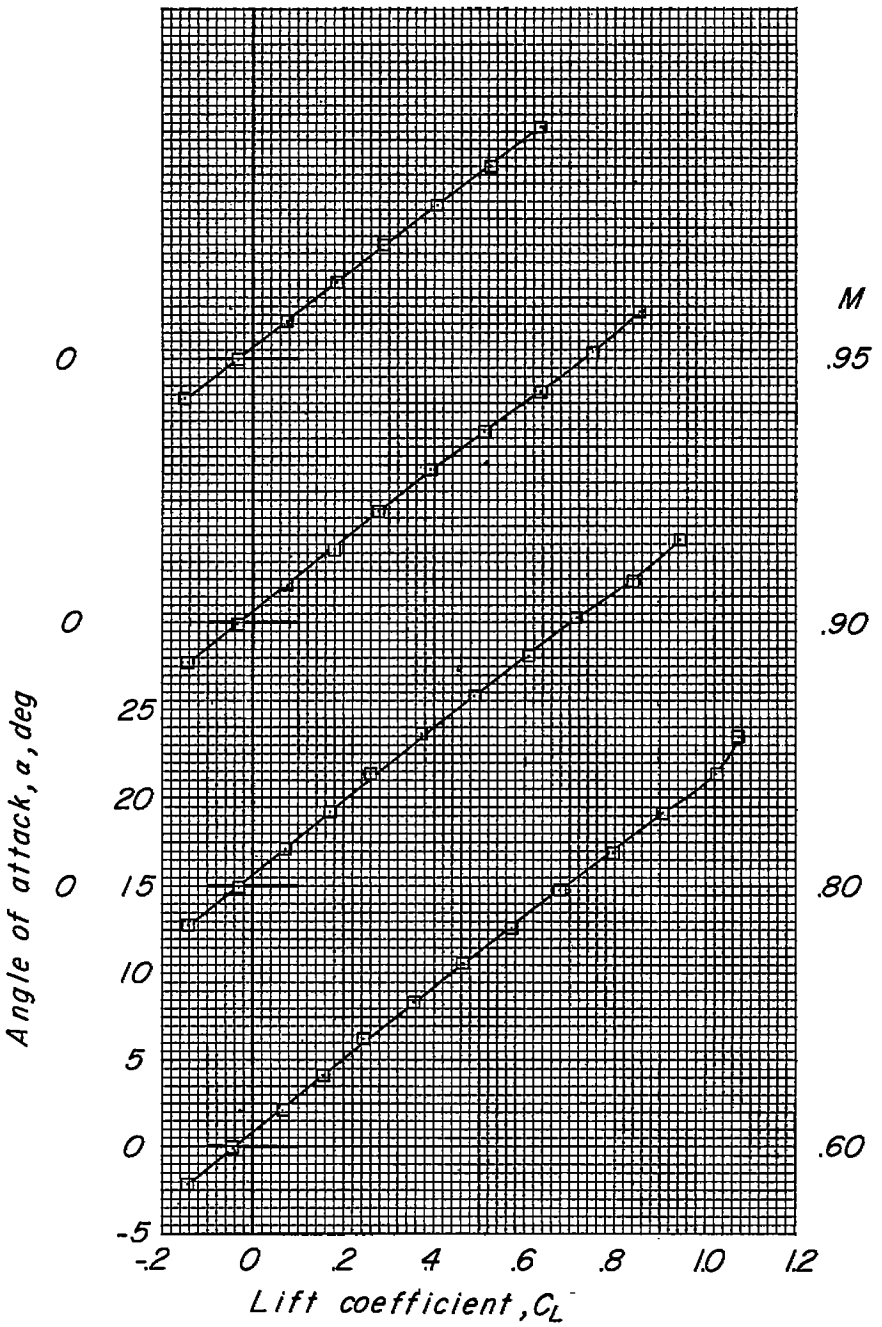

(a) Variation of α with C_L.

Figure 9.- Longitudinal characteristics of wing-fuselage model with cambered and twisted wing and indented (M = 1.4) area-rule body. Fixed transition.

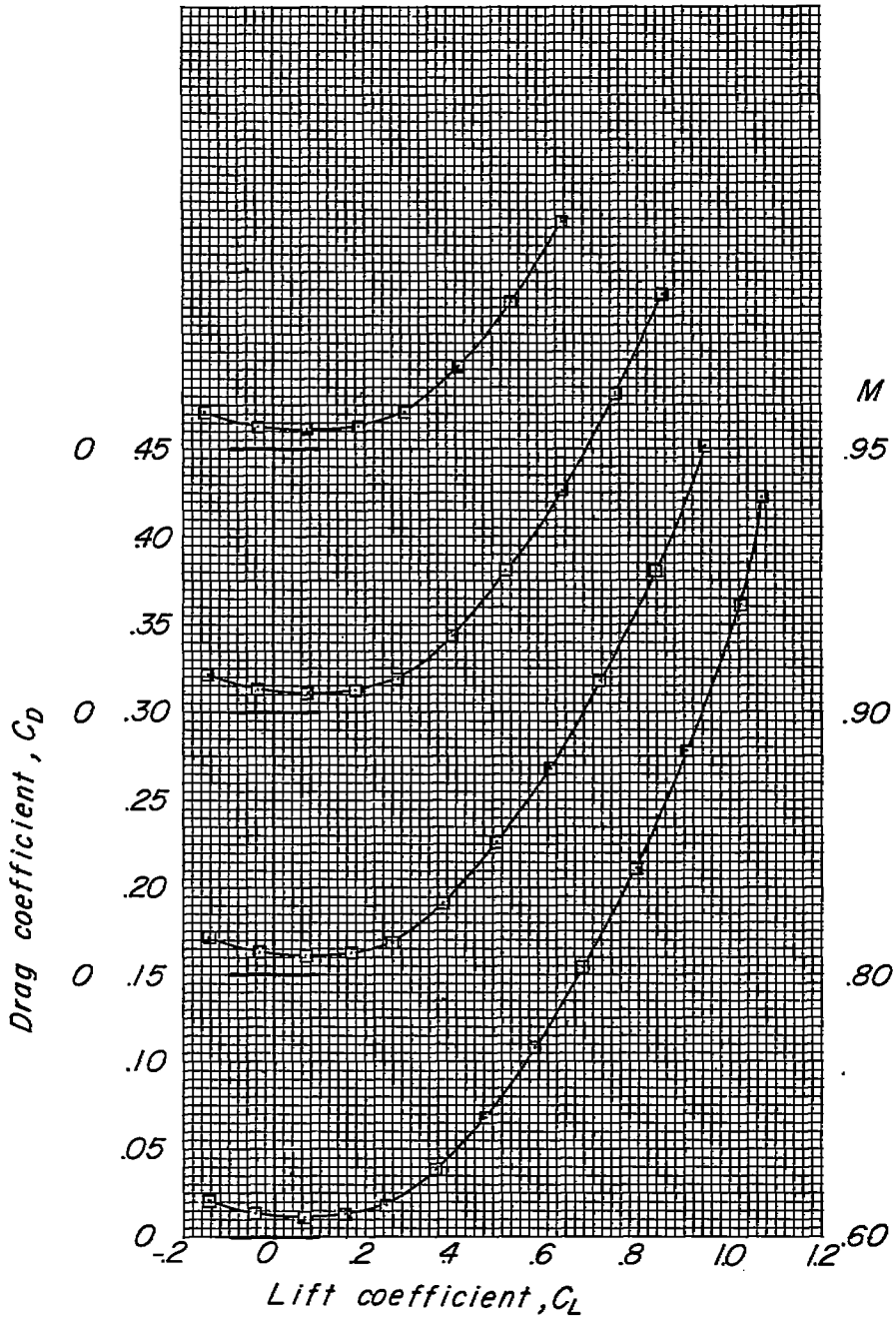

(b) Variation of C_D with C_L.

Figure 9.- Continued.

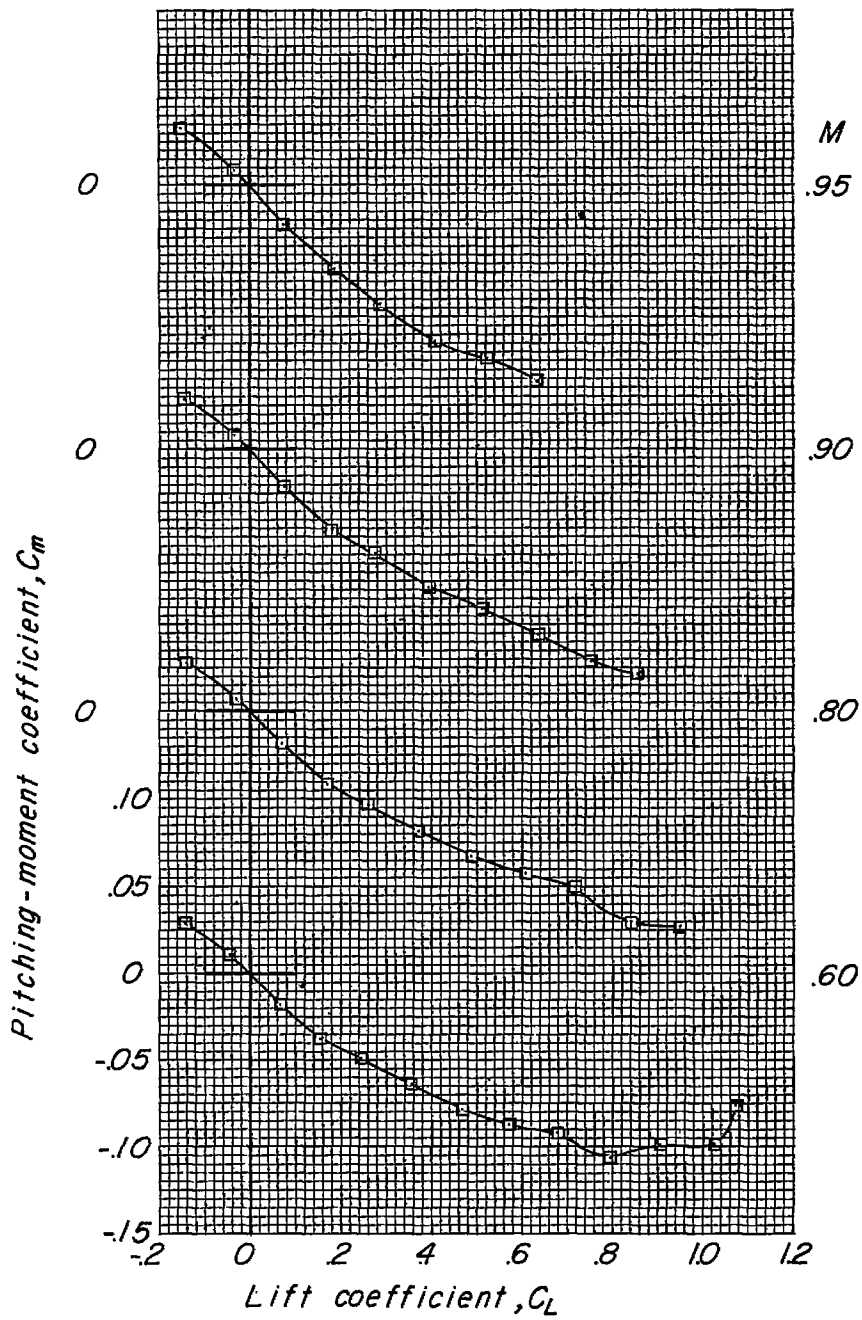

(c) Variation of C_m with C_L.

Figure 9.- Concluded.

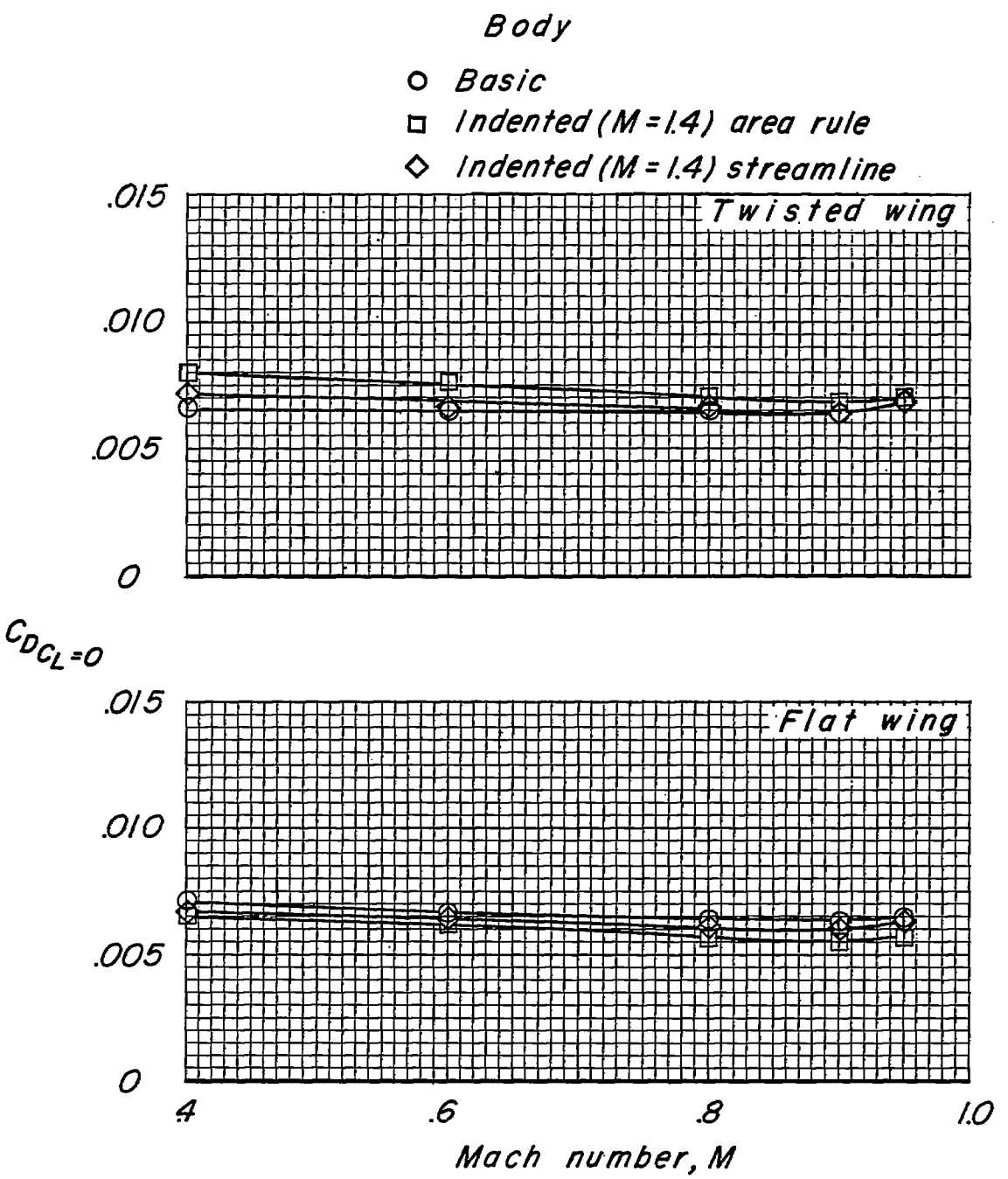

Figure 10.- Effect of body indentation on the variation of drag at zero lift with Mach number. Free transition.

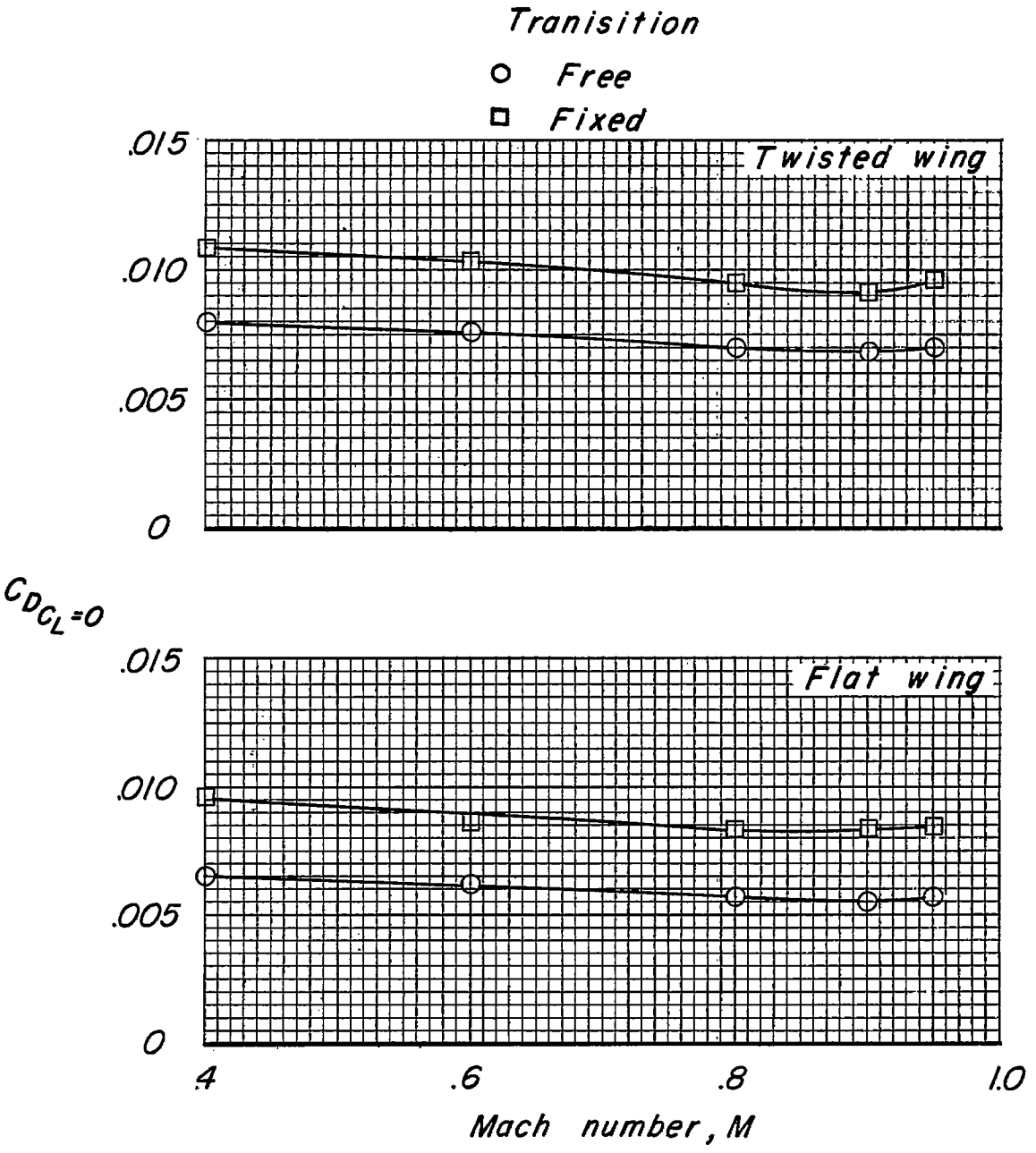

Figure 11.- Effect of transition on the variation of drag at zero lift with Mach number of the model with the indented (M = 1.4) area-rule body.

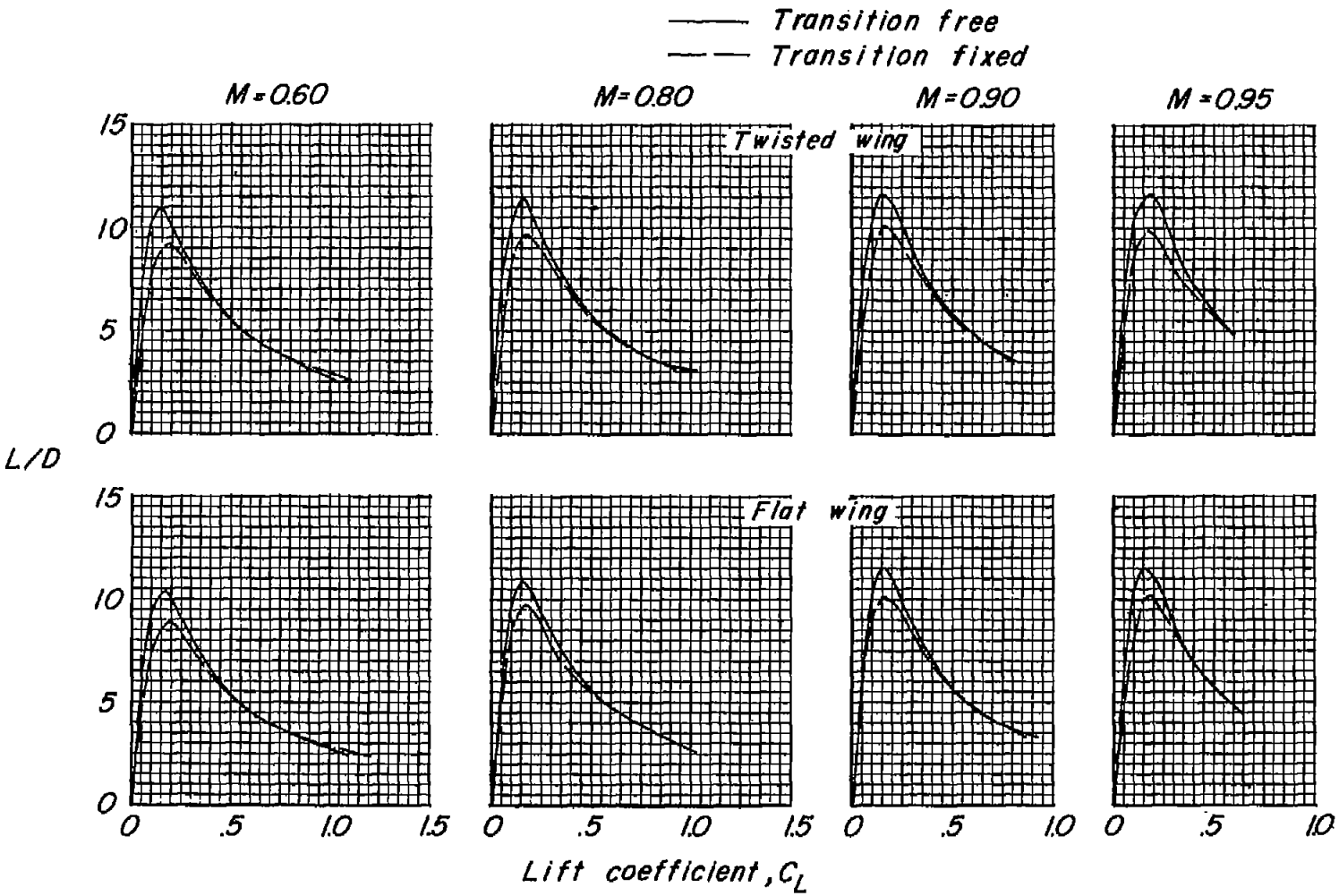

Figure 12.- Effect of transition on the variation of lift-drag ratio with lift coefficient of the model with the indented (M = 1.4) area-rule body.

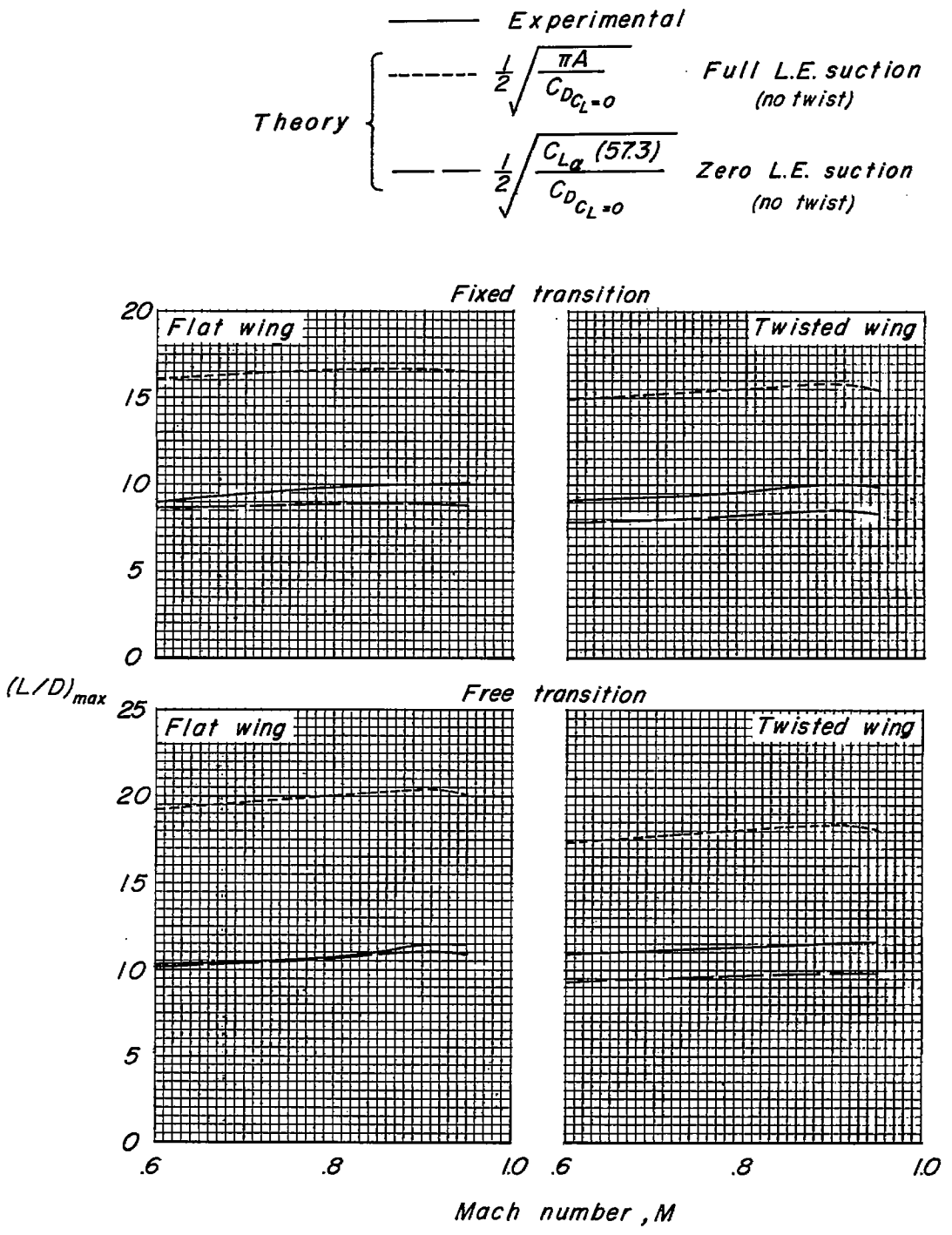

Figure 13.- The variation of maximum lift-drag ratio with Mach number of the model with the indented (M = 1.4) area-rule body.

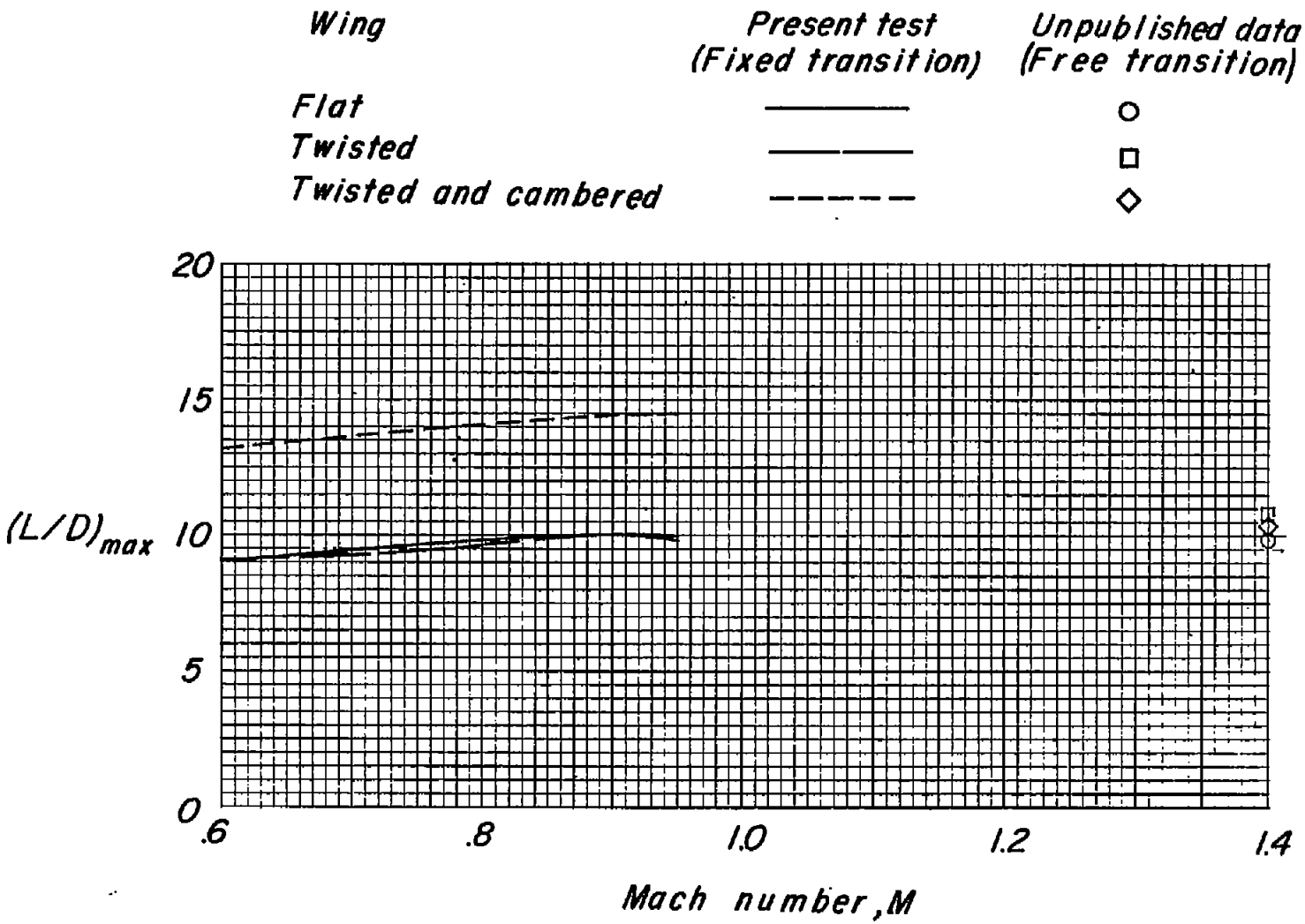

Figure 14.- Effect of twist and of camber and twist on the maximum lift-drag ratio with Mach number for the model with the indented (M = 1.4) area-rule body. Fixed transition.

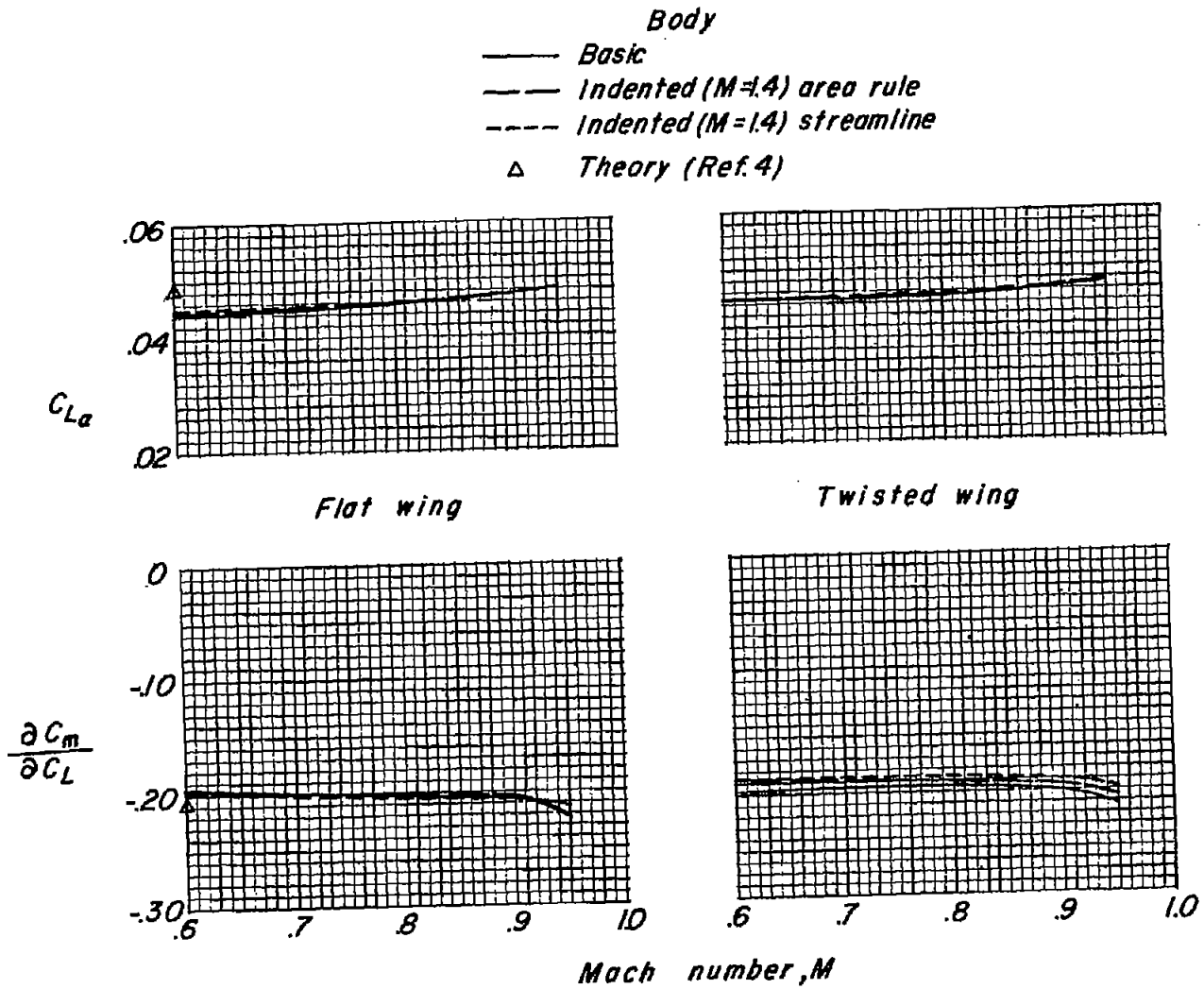

Figure 15.- The effect of body indentation on the variation of lift-curve slope and static margin with Mach number.